NATIONAL AERONAUTICS AND SPACE ADMINISTRATION

Technical Report 32-986

A Theory for the Design of One-Way and Two-Way Phase-Coherent Communication Systems

Phase-Coherent Tracking Systems

W. C. Lindsey

JET PROPULSION LABORATORY
CALIFORNIA INSTITUTE OF TECHNOLOGY
PASADENA, CALIFORNIA

July 15, 1969

NATIONAL AERONAUTICS AND SPACE ADMINISTRATION

Technical Report 32-986

A Theory for the Design of One-Way and Two-Way Phase-Coherent Communication Systems

Phase-Coherent Tracking Systems

W. C. Lindsey

JET PROPULSION LABORATORY
CALIFORNIA INSTITUTE OF TECHNOLOGY
PASADENA, CALIFORNIA

July 15, 1969

Prepared Under Contract No. NAS 7-100
National Aeronautics and Space Administration

Preface

The work described in this report was performed by the Telecommunications Division of the Jet Propulsion Laboratory.

Contents

Contents (contd)

Contents (contd)

Chapter 7. Diversity Combining to Improve Radio-Frequency Phase and Doppler Measurements in One-Way and Two-Way Coherent Communication Systems

Figures

Contents (contd)

Figures (contd)

Abstract

This report presents a mathematical theory for use in the design of phase-coherent tracking systems for deep-space applications. The theory is sufficiently general to include the design of both one-way and two-way systems. Because phase-locked loops, which comprise the heart of such systems, are nonlinear devices, this working theory is based on the nonlinear phase-locked-loop theory. From the working theory and certain aspects of the nonlinear theory, an approximate model that takes into consideration the nonlinear effects associated with phase-locked loops has been developed. This approximate model is predicated and justified on the basis of measurements in the laboratory, and, for all practical purposes, appears to fall within the region that constitutes a check between theory and practice. The model also accommodates the use of band-pass limiters in the system.

Chapter 1
Space-Communication Network Concepts

I. Introduction

Before any attempt to assemble words, formulas, notation, and design figures that aid the communications engineer in designing a practical communication system for deep-space applications, the portion of the overall communication network involved in the theory must be defined.

The relative success of a deep-space mission depends upon the ability to collect useful scientific and engineering data during all of its phases. This flow of data requires a very precise communication network such as the Deep Space Network (DSN), which is designed to communicate with, and permit control of, spacecraft (SC) designed for deep-space exploration. The main elements of the DSN are the Deep Space Instrumentation Facility (DSIF), composed of space communication and tracking stations around the world; the Space Flight Operations Facility (SFOF), which is the command and control center located at JPL in Pasadena, California; and the Ground Communication System (GCS), which connects all parts of the DSN by voice, teletype lines, and high-speed data lines. These elements of the DSN are illustrated in simplified form in Fig. 1-1. The flow of information in the DSN consists of several data types,

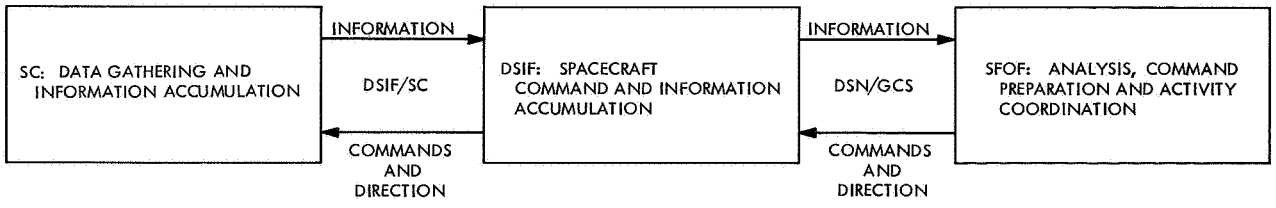

Fig. 1-1. Generic model of the Deep Space Network

including tracking data to and from the spacecraft, commands, telemetry, and administrative information.

Tracking data, giving the position and velocity of the spacecraft, is the result of data processing done at the DSIF Deep Space Stations. The flow of this data through the Network is a pattern of unsteady arrivals and retransmissions at different points in time during any mission.

Command data transmitted to the spacecraft is generated usually at the SFOF; this data controls the spacecraft. The flow of data is unsteady and conveyed to the spacecraft via a GCS/DSIF communication link.

Telemetry data flows continuously from the spacecraft; it is received and processed at the DSIF sites, and transmitted to the SFOF by means of the GCS. This information received at the SFOF pertains to the performance and condition of the spacecraft.

Administrative data is stochastic flow because the time between separate arrivals of the data to the network and the demand placed on the particular channel by each of these arrivals are random quantities. This type of data includes voice channels, reporting conditions, and approvals.

The exposition to follow is concerned with the design of the DSIF/SC communication link. The knowledge base of this exposition is contained in the bibliography at the end of this chapter; the reader should have a basic understanding of this material. Because the spacecraft and communication stations are not, for the purpose of this report, specific, the spacecraft will be referred to as the "vehicle system," and the DSIF as the "reference system." The vehicle-to-reference communication link may be further separated into two radio links, the "uplink," which is used for transmission to the vehicle, and the "downlink," which is used for transmission back to the reference system. Both the uplink and the downlink can be used for tracking purposes (i.e., determination of the vehicle orbit or trajectory).

That portion of the vehicle-to-reference system communication link considered here is depicted in Fig. 1-2. The inputs to the reference-system transmitter consist of discrete and quantitative commands and tracking information; the outputs of the vehicle system consist of discrete and quantitative commands, noise, and tracking information. Inputs to the vehicle-system transmitter include spacecraft performance data, scientific data, and tracking information. The reference-system outputs are telemetry data (both spacecraft performance and scientific data), tracking data, and noise.

The development of a theory for the design of the vehicle-to-reference communication link can be simplified by concocting an analytical model of the system that is mathematically tractable. From this model, a tractable theory can be developed that includes the effects of such nonlinear system elements as the phase-locked loop (PLL) and the band-pass limiter (BPL). The approach taken to formalize the theory is illustrated in Fig. 1-3. Here, and in the chapters that follow, exposition of the system theory will follow the four-part buildup shown in this figure.

The first cut at any system design would, on the basis of the inputs (e.g., transmitter power and antenna gain), predicate the design on the basis of the linear PLL

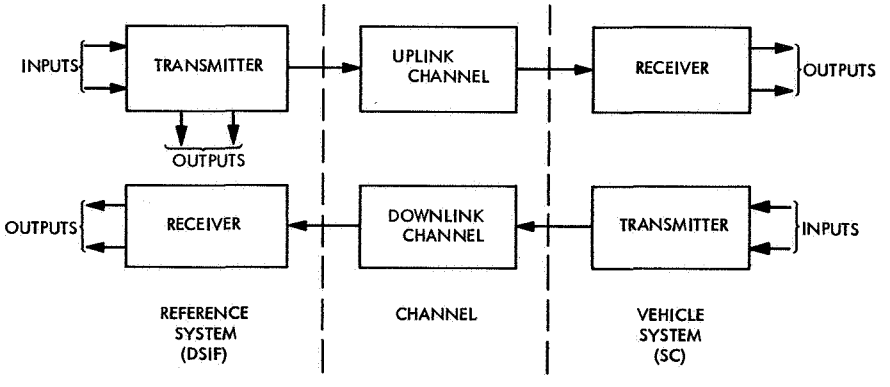

Fig. 1-2. DSIF-to-SC and SC-to-DSIF communication links

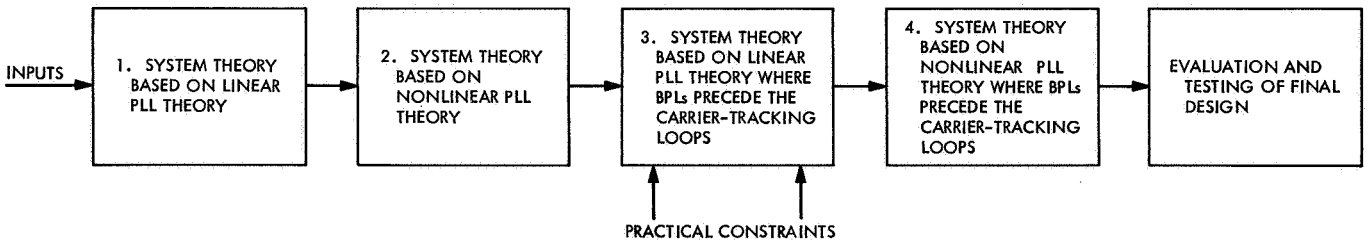

Fig. 1-3. Buildup of a working theory for the design of deep-space communication systems

theory. Because the PLL is inherently a nonlinear system, a check could be made using the nonlinear PLL theory to determine where such a system would actually operate in practice. In the third step of design, several practical constraints, the introduction, for example, of BPLs before the carrier-tracking PLL, must be considered. Thus, the design could be re-established using part 3 of Fig. 1-3; to effect the final design, part 4 would be used. The final step, testing and evaluation of system performance, would be performed in the laboratory. The laboratory measurements could then be compared with those predicted by part 4 of the system theory. With design, testing, and evaluation completed, the system is ready for use in a deep-space mission.

II. The Problem

The design, testing, and evaluation of performance of the DSIF/SC communication system described above requires a measurement of system performance that, in accordance with communication theory, will provide "optimum" solutions to system design problems.

The definition of "optimum" is determined by which of the three system functions (i.e., tracking, telemetry, or command) the communication engineer considers most important. In any deep-space mission, the level of importance of these functions changes with respect to the position of the spacecraft relative to the earth (i.e., the time after launch), thus making any definition of "optimum" difficult to defend. Immediately after launch, for example, the tracking function assumes priority. Near midcourse maneuver, the ability to send commands to the vehicle and have them detected and executed correctly is of prime importance. After the midcourse maneuver, tracking again becomes the most important function because the spacecraft trajectory must be redetermined with great accuracy. Telemetry is important through all phases of a deep-space mission. At encounter, final descent, or terminal maneuver, all three communication system functions are equally important. The failure of any one of the functions may prove costly, or even catastrophic to the mission.

Thus, the definition of "optimum" depends upon that part of the overall design treated. In tracking system design, optimum could mean selection of those system parameters that minimize the error in doppler measurements. In telemetry- or command-system design, optimum could mean the apportionment of the total transmitter power between the carrier and one or more sidebands to minimize the probability of error. A good, overall system design, therefore, requires a thorough understanding of all three functions. Tractable mathematical solutions sometimes require the freezing of certain system variables or parameters (such as the ratio of the bandwidth of the spacecraft's carrier-tracking loop to that of the ground receiver), and compromises made among others. The addition of such a practical constraint as preceding the carrier-tracking loops with BPLs greatly complicates the design problem, of course, but the need of BPLs in any practical system has long been recognized by design engineers. Thus, the selection of an optimum criterion depends to a large extent upon what is practical, and the current state of the communication art (e.g., the level of development of such system components as low-noise amplifiers, masers, antennas, IF amplifiers, and modulators). For these reasons, and because the mathematical model for such a system is complicated, design of a practical communication system must proceed by treating each system function separately, while working toward the integration of all functions as a whole.

This description of the approach used in manipulating the mathematical model defines the goals in the design of a deep-space communication system; theoretical development may now proceed.

Bibliography

Baghdady, E. J., *Lectures on Communication System Theory.* McGraw-Hill Book Company, Inc., New York, 1961.

Balakrishnan, A. V., *Advances in Communication Systems.* Academic Press Inc., New York, 1965.

Balakrishnan, A. V., *Space Communications.* McGraw-Hill Book Company, Inc., New York, 1963.

Bennett, W. R., and Davey, J. R., *Data Transmission.* McGraw-Hill Book Company, Inc., New York, 1965.

Black, H. S., *Modulation Theory.* D. Van Nostrand Company, Inc., Princeton, New Jersey, 1953.

Cunningham, W. J., *Nonlinear Analysis.* McGraw-Hill Book Company, Inc., New York, 1958.

Davenport, W. B., and Root, W. L., *An Introduction to the Theory of Random Signals and Noise.* McGraw-Hill Book Company, Inc., New York, 1958.

Dynkin, E. B., and Brown, D. E., *Theory of Markov Processes.* Prentice-Hall, Inc., Englewood Cliffs, New Jersey, 1961.

Golomb, S. W., et al., *Digital Communications With Space Applications.* Prentice-Hall, Inc., Englewood Cliffs, New Jersey, 1964.

Hancock, J. C., *An Introduction to the Principles of Communication Theory.* McGraw-Hill Book Company, Inc., New York, 1961.

Hancock, J., and Wintz, P., *Signal Detection Theory.* Prentice-Hall, Inc., Englewood Cliffs, New Jersey, 1966.

Harman, W. H., *Principles of the Statistical Theory of Communication.* McGraw-Hill Book Company, Inc., New York, 1963.

Helstrom, C. W., *Statistical Theory of Signal Detection.* Pergamon Press, New York, 1960.

Kailath, T., *Statistical Decision Theory.* Prentice-Hall, Inc., Englewood Cliffs, New Jersey (in press).

Kleinrock, L., *Communication Nets.* McGraw-Hill Book Company, Inc., New York, 1964.

Middleton, D., *An Introduction to Statistical Communication Theory.* McGraw-Hill Book Company, Inc., New York, 1960.

Schwartz, M., *Information Transmission, Modulation, and Noise.* McGraw-Hill Book Company, Inc., New York, 1959.

Stiffler, J. J., *Theory of Synchronous Communications.* Prentice-Hall, Inc., Englewood Cliffs, New Jersey (in press).

Stratonovich, R. L., *Topics in the Theory of Random Noise.* Gordon and Breach, Science Publishers, Inc., New York, 1963.

Bibliography (contd)

The Theory of Optimum Noise Immunity. McGraw-Hill Book Company, Inc., New York, 1959.

Viterbi, A. J., *Principles of Coherent Communications.* McGraw-Hill Book Company, Inc., New York, 1966.

Wainstein, L. A., and Zubakov, V. D., *Extraction of Signals From Noise.* Prentice-Hall, Inc., Englewood Cliffs, New Jersey, 1962.

Weber, C. L., *Elements of Detection and Signal Design.* McGraw-Hill Book Company, Inc., New York, 1968.

Wozencraft, J. M., and Jacobs, I. M., *Principles of Communication Engineering.* John Wiley & Sons, Inc., New York, 1965.

Chapter 2
The Second-Order Phase-Locked Loop

Certain concepts pertinent to the behavior of phase-locked loops and necessary to the discussions that follow are presented in this section; however, a complete exposition of the theory, design, and performance of PLLs is unnecessary. A thorough and lucid treatment of various aspects of the behavior of PLLs in the presence of noise is given in Refs. 2-1 through 2-6.

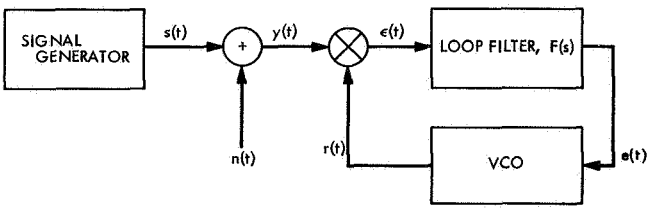

Fig. 2-1. Simplest form of a PLL receiver

I. Fundamental Operation

Phase-locked loops are widely used in radio engineering and automation, in synchronizing devices and for automatic frequency control. The theory of operation can be elucidated using the simplest functional block diagram, Fig. 2-1. The harmonic oscillations $s(t) = \sqrt{2P} \times \sin(\omega_0 t + \theta)$ of the signal generator, and $r(t) = \sqrt{2} \cos \times (\omega_0 t + \hat{\theta})$ of the voltage-controlled oscillator (VCO) output act on the multiplier to produce the voltage $\epsilon(t)$. This voltage, $\epsilon(t)$, depends upon the difference between the phase and frequency of the signals $r(t)$ and $s(t)$, and upon the additive noise $n(t)$. The resulting signal $\epsilon(t)$, after filtering by the loop filter $F(p)$, changes the output frequency and phase of the VCO (synchronized generator) to coincide, in the absence of noise, with the frequency and phase of the signal generator. Even in the absence of external noise, fluctuations due to the circuit elements occur in PLL operation. In the signal-to-noise ratio region of currently expected PLL operations, the effects of these internal fluctuations are small in comparison with the effects produced by the additive noise $n(t)$; hence, in what follows, any instabilities in the VCO (Refs. 2-1, 2-2, and 2-3) are neglected. By a slight modification of the PLL theory, the VCO instabilities may be included.

II. Essentials From Linear PLL Theory

The received waveform $y(t)$ is defined by

$$y(t) = \sqrt{2P} \sin [\omega_0 t + \theta(t)] + n(t) \qquad (2\text{-}1)$$

where

$$n(t) = x_1(t) \cos(\omega_0 t + \theta) + x_2(t) \sin(\omega_0 t + \theta) \qquad (2\text{-}2)$$

represents the additive noise process. Both x_1 and x_2 are assumed to be statistically independent, stationary, white Gaussian noise processes of the single-sided spectral density N_0 W/Hz. The reference signal $r(t)$ at the output of the VCO is presumed to be a sinusoid, the instantaneous frequency of which is related to the input control voltage $e(t)$ through the relationship

$$\hat{\theta}(t) = K \int^t e(\tau) d\tau \tag{2-3}$$

and

$$r(t) = \sqrt{2} \cos [\omega_0 t + \hat{\theta}(t)] \tag{2-4}$$

Note that the entire gain of the loop is grouped into the gain of the VCO.

Thus the product of the input $y(t)$ and $r(t)$ may be shown to be related, in operational form, to the phase error $\phi(t)$ by

$$\begin{aligned} \phi(t) &= \theta(t) - \hat{\theta}(t) \\ &= \theta(t) - \frac{KF(p)}{p} [\sqrt{P} \sin \phi + n'(t)] \end{aligned} \tag{2-5}$$

where all double-frequency terms have been neglected because neither the loop filter $F(p)$ nor the VCO will respond significantly to them. In Eq. (2-5), the constant K is the open-loop gain (p. 17 of Ref. 2-1) and p is the Heaviside operator. Further, under certain physically justifiable conditions (Refs. 2-1 and 2-4), it may be shown that $n'(t)$, consisting of two terms, is white Gaussian phase noise with the same spectral density as that of the original additive process $n(t)$. Thus, in a study of receiver structure from input to output, Eq. (2-5) provides the pertinent quantities, and the PLL may be conveniently represented by the block diagram of Fig. 2-2.

If the loop is linearized (i.e., assume $\sin \phi \approx \phi$), the closed-loop transfer function $H(p)$ of the PLL may be

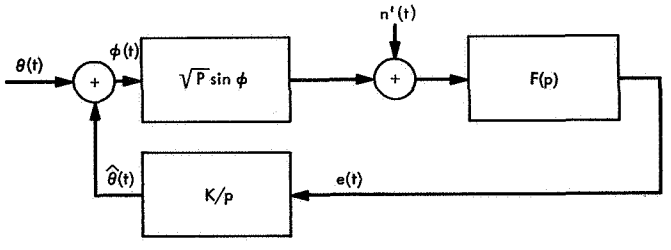

Fig. 2-2. Exact equivalent receiver

written by inspection from Fig. 2-2 as

$$H(p) = \frac{F(p) K \sqrt{P}}{s + F(p) K \sqrt{P}} \tag{2-6}$$

Therefore, the linearized closed-loop transfer function is specified once the loop filter is determined. In practice, the loop filter that corresponds to the one generally employed for carrier-tracking purposes is given by

$$F(p) = \frac{1 + \tau_2 p}{1 + \tau_1 p} \tag{2-7}$$

Substituting Eq. (2-7) into Eq. (2-6), we have

$$H(p) = \frac{1 + \tau_2 p}{1 + \left(\tau_2 + \dfrac{1}{K\sqrt{P}}\right) s + \left(\dfrac{\tau_1}{K\sqrt{P}}\right) s^2} \tag{2-8}$$

In practice, the variance of the phase error is an important parameter. For the simple linear model, the variance of the phase error is given by

$$\sigma_\phi^2 = \frac{N_0 W_L}{2P} = \frac{N_0}{2P} \left[\frac{1 + \dfrac{K\tau_2^2 \sqrt{P}}{\tau_1}}{2\tau_2 \left(1 + \dfrac{1}{K\tau_2 \sqrt{P}}\right)} \right] \tag{2-9}$$

where

$$W_L = \frac{1}{2\pi j} \int_{-j\infty}^{j\infty} |H(s)|^2 \, ds \tag{2-10}$$

is the loop bandwidth defined by the linear PLL theory.

If we define

$$r = K \tau_2^2 \frac{\sqrt{P}}{\tau_1} \tag{2-11}$$

then, from Eqs. (2-8) and (2-10), we have

$$W_L \cong \frac{r+1}{2\tau_2} \tag{2-12}$$

when $r\tau_1 \gg \tau_2$ (the case of greatest interest in practice). Thus Eq. (2-8) becomes

$$H(p) = \frac{1 + \left(\dfrac{r+1}{2W_L}\right) p}{1 + \left(\dfrac{r+1}{2W_L}\right) p + \dfrac{1}{r} \left(\dfrac{r+1}{2W_L}\right)^2 p^2} \tag{2-13}$$

which *is* the form of greatest interest in the exposition that follows.

III. Nonlinear PLL Theory

In a coherent communication system, a main function of the PLL is tracking a radio-frequency carrier. This section, therefore, presents significant results from the nonlinear PLL theory that will be useful in the development of the theory of coherent telemetry, command, and tracking systems.

The most promising analytical approach in developing an exact nonlinear PLL theory is based on the Fokker–Planck method (Refs. 2-2 through 2-6). This method leads to an expression for the probability distribution of the nonstationary phase error that, in the steady state, gives an unbounded variance. This behavior of the variance is, of course, a result of the cycle-slipping phenomenon associated with PLLs. However, Viterbi (Ref. 2-4) and Tikhonov (Refs. 2-2 and 2-3) were successful in applying this method to the analysis of the first-order loop by recognizing that the phase-error-density-reduced modulo 2π is stationary in the steady state and possesses a bounded variance. Extension of the Fokker–Planck method to the second-order PLL [i.e., a loop filter of the proportional-plus-integral control type, Eq. (2-7)] is given in Refs. 2-5 and 2-6. The theory developed there suggests the possibility of approximating the second-order-loop phase-error density by the more tractable results obtained from analysis of the first-order loop. Demonstrating the validity of using the expression for the first-order-loop phase-error density in describing the statistics of the phase error in a second-order loop is the intent of the discussion that follows.

The signal-plus-noise model of specific interest may be briefly characterized: the input signal to the PLL is assumed to be an unmodulated sine wave of fixed phase θ, frequency ω_0, power P in watts, plus additive white Gaussian noise of single-sided spectral density N_0 W/Hz as described in Eq. (2-1).

A particular mechanization of the proportional-plus-integral control-loop filter is illustrated in Fig. 2-3; the transfer function of this filter is given by Eq. (2-7). If we equate the two time constants τ_1 and τ_2, the probability distribution of the phase error is given by

$$p_1(\phi) = \frac{\exp(\alpha_1 \cos\phi)}{2\pi I_0(\alpha_1)}, \qquad |\phi| \leq \pi \tag{2-14}$$

where $\phi(t) \triangleq \theta(t) - \hat{\theta}(t)$. This distribution is the result obtained by Viterbi (Ref. 2-4) and Tikhonov (Refs. 2-2 and 2-3) for the first-order loop. In particular, $\alpha_1 = 4P/(KN_0\sqrt{P})$ is the signal-to-noise ratio in the bandwidth of the linearized first-order loop. We now define an equivalent parameter α as the signal-to-noise ratio in the bandwidth of the linearized second-order loop, i.e.,

$$\alpha \triangleq \frac{2P}{N_0 W_L} \tag{2-15}$$

where, as defined in Eq. (2-12),

$$W_L = \frac{1}{2\pi j}\int_{-j\infty}^{j\infty} |H(s)|^2\, ds$$

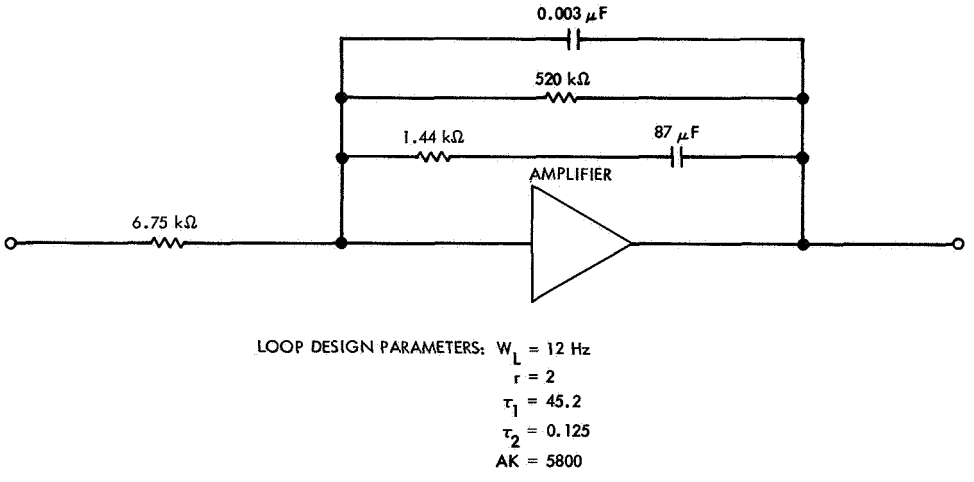

Fig. 2-3. Loop filter mechanization

and $H(s)$ is the closed-loop transfer function of the linearized second-order loop. Replacing the parameter α_1 in Eq. (2-14) by α of Eq. (2-15), we have

$$p(\phi) = \frac{\exp(\alpha \cos \phi)}{2\pi I_0(\alpha)}, \qquad |\phi| \leq \pi \quad (2\text{-}16)$$

The validity of using Eq. (2-16) to represent the statistical properties of the phase error in a second-order loop can be verified by comparing the equation graphically with an experimentally derived distribution. The closeness of the equation's approximation to the statistical properties is clearly evident from Fig. 2-4 where the analytical distribution (solid curve) is superimposed over the experimental distribution (point plot) for various values of α in the range 6.5 dB $> \alpha >$ 0 dB. The cumulative distributions of the measured phase error are shown in Fig. 2-5 for the same values of α. As shown in this figure, the probability of the loop-losing lock is extremely small when $\alpha > 6.41$ dB. It is also evident from the cumulative distributions that the phase-error density tends to become uniform for low signal-to-noise ratios. In Fig. 2-6, the variance of the phase error computed from the linear model and from Eq. (2-13) is compared with the variance of the measured phase error over the range of signal-to-noise ratio $0 < \alpha < 6.5$ dB. In subsequent chapters, these results will be used to characterize the nonlinear behavior and performance of one-way and two-way phase-coherent communication systems.

IV. Dynamics of Second-Order PLLs (Fokker–Planck Analysis)

Recent results relative to the statistical dynamics of the phase-error process in second-order PLLs (Ref. 2-6) justify the conclusions presented in Section III of this

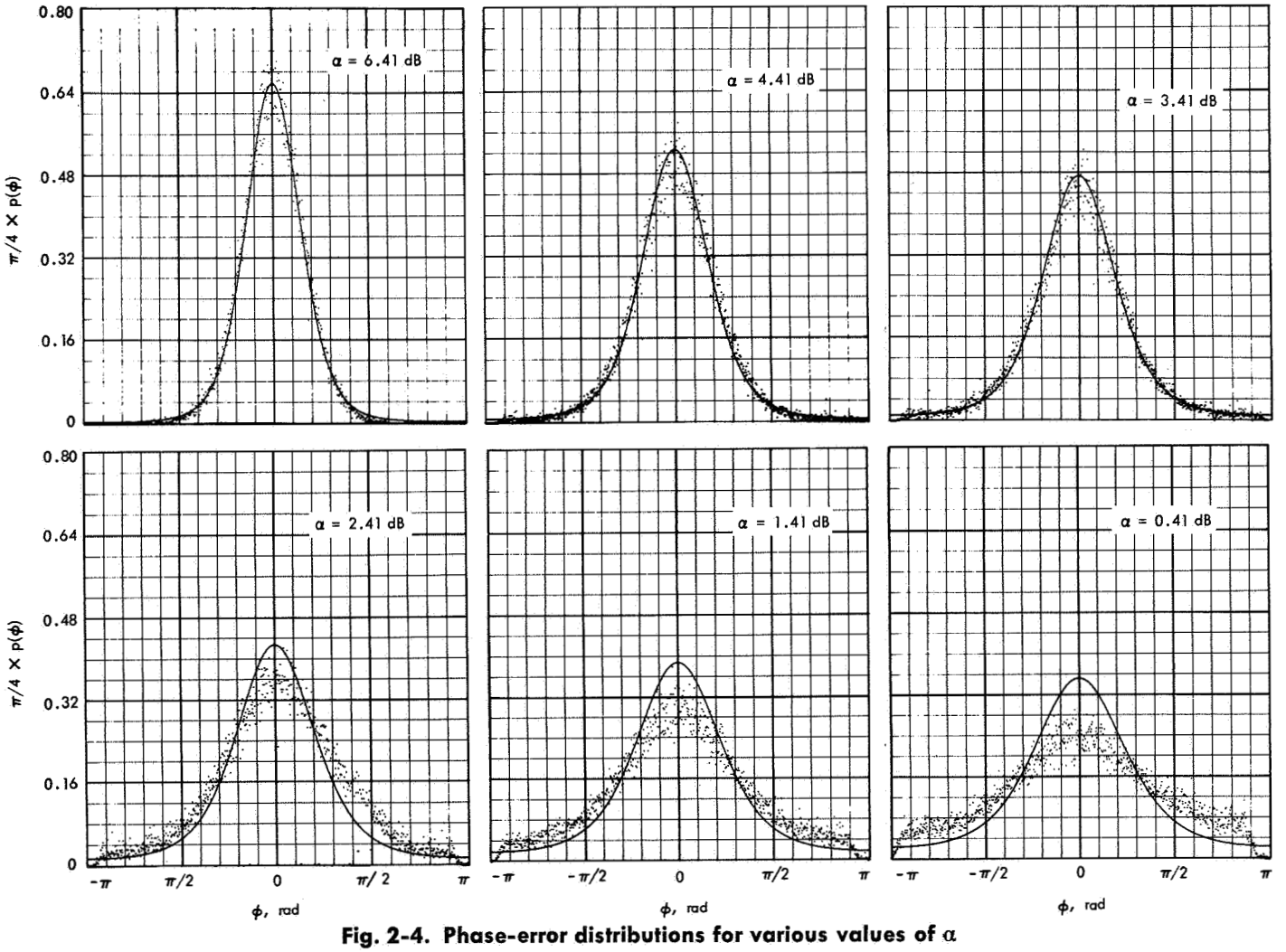

Fig. 2-4. Phase-error distributions for various values of α

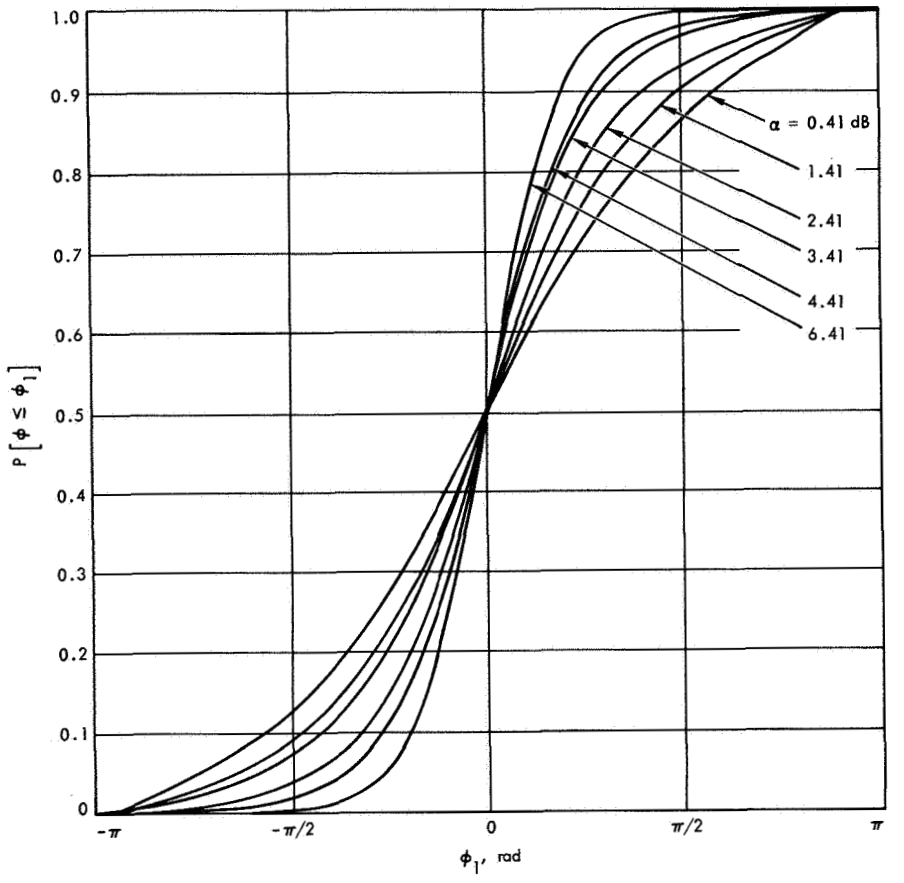

Fig. 2-5. Cumulative distribution of the measured phase error

chapter. The problem that led to these results concerns the actual phase-error process $\tilde{\phi}(t)$.

The actual phase-error process $\tilde{\phi}(t)$ in a PLL system undergoes diffusion much like a particle in Brownian motion; hence, the variance of the phase error becomes infinite in the steady state. Previous work (Refs. 2-2 and 2-3) on determining the probability distribution of the phase error in the steady state of a first-order loop was accomplished by reducing the phase-error modulo 2π to a $\phi(t)$ process. Because such a reduction ignores the number of cycles that have slipped with the passage of time, diffusion of the phase error takes place. For finding telemetry error probabilities, this reduction is all that is needed; for estimating tracking accuracy, however, the $\tilde{\phi}(t)$ process itself must be studied.

To completely describe the $\tilde{\phi}(t)$ process, one must account for that component of the variance of the phase error that causes diffusion, i.e., cycle slipping. Cycle slipping is perhaps best described by evaluating the diffusion coefficient, i.e., the rate at which the variance of the phase error is approaching infinity, and combining this component of the variance in some way with the variance of the phase-error-reduced modulo 2π.

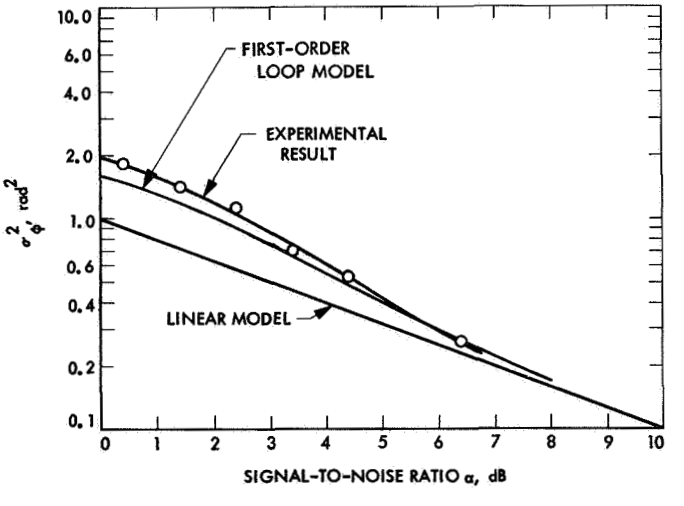

Fig. 2-6. Experimental and analytical results relative to the variance of the phase error

For a second-order loop, an approximate solution is given below for the steady-state distribution of the phase-error-reduced modulo 2π; the regions of validity for this solution are established by comparing it to experimental results. In addition, approximate formulas are given for (1) the diffusion coefficient of the phase-error process, (2) the expected values of the time intervals between cycle-slipping events, (3) the expected number of cycles slipped per unit of time, (4) the expected number of cycles slipped "to the right" and "to the left," (5) the expected value of the phase-error rate in the steady state, and (6) the mean time to the first slip. In the limit as the system damping approaches infinity, the results of these formulas are valid for the first-order loop.

A. Loop Model and Phase-Error-Density-Reduced Modulo 2π

For a PLL system with loop filter

$$F(s) = \frac{1 + \tau_2 s}{1 + \tau_1 s} \tag{2-17}$$

it has been recently shown (Ref. 2-6) that the probability distribution of the phase-error-reduced modulo 2π is given a good approximation by

$$p(\phi) = \frac{\exp(\beta\phi + \alpha\cos\phi)}{4\pi^2 \exp(-\pi\beta)\,|\,I_{j\beta}(\alpha)\,|^2} \times \int_{\phi}^{\phi+2\pi} \exp(-\beta x - \alpha\cos x)\,dx \tag{2-18}$$

where $I_v(x)$ is the imaginary Bessel function of order v and argument x and ϕ belongs to any interval of width 2π centered about any lock point $2n\pi$; n is any integer. The parameters α and β that characterize Eq. (2-18) are related to the various system parameters through

$$\left.\begin{aligned} F_1 &= \frac{\tau_2}{\tau_1}; \qquad \Omega_0 = \omega - \omega_0 \\ \beta &= \left(\frac{r+1}{r}\right)^2 \frac{\rho}{2W_L}\left[\Omega_0 - AK(1 - F_1)\,\overline{\sin\phi}\right] \\ \alpha &= \left(\frac{r+1}{r}\right)\rho - \frac{1 - F_1}{r\,\sigma_G^2} \end{aligned}\right\} \tag{2-19}$$

where $G = \sin\phi - \overline{\sin\phi}$, the superbar denotes statistical average, Ω_0 represents the amount of loop detuning or frequency offset, ρ is the signal-to-noise ratio in the loop bandwidth, and $W_L \approx (r+1)/2\tau_2$ if $r\,\tau_1 \gg \tau_2$. The parameter $r = AK\,\tau_2^2/\tau_1 = \sqrt{\zeta/4}$ where ζ is the "loop damping," and AK represents open loop gain. Moments of $\sin n\phi$ and $\cos(n\phi)$ are given by (Ref. 2-6)

$$\left.\begin{aligned} \overline{\sin(n\phi)} &= Im\left[\frac{I_{n-j\beta}(\alpha)}{I_{-j\beta}(\alpha)}\right]; \qquad \overline{\cos(n\phi)} = Re\left[\frac{I_{n-j\beta}(\alpha)}{I_{-j\beta}(\alpha)}\right] \\ \overline{\cos^2\phi} &= \frac{1 + \cos 2\phi}{2}; \qquad \overline{\sin^2\phi} = \frac{1 - \overline{\cos 2\phi}}{2} \end{aligned}\right\} \tag{2-20}$$

with

$$\sigma^2_{\sin\phi} = \overline{\sin^2\phi} - (\overline{\sin\phi})^2$$

Re [•] denotes the real part of the quantity in the brackets. It is clear from Eqs. (2-18) and (2-20) that $p(\phi)$ will be symmetric when the loop is designed such that $\beta = 0$.

The expected value of the phase-error can be found from Eq. (2-18) and the well known Bessel function expansions of $\exp(\pm x\cos\phi)$. Without going into details (see Ref. 2-6), we have

$$\bar{\phi} = \int_{-\pi}^{\pi} \phi\,p(\phi)\,d\phi = \frac{2\sinh\pi\beta}{\pi\,|\,I_{j\beta}(\alpha)\,|^2} \sum_{m=1}^{\infty} \frac{m\,I_m(\alpha)}{m^2 + \beta^2}\left[\frac{I_0(\alpha)}{m} + \frac{I_m(\alpha)}{4m} + \sum_{\substack{k=1 \\ k\neq m}}^{\infty} \frac{2m(-1)^k I_k(\alpha)}{m^2 - k^2}\right] \tag{2-21}$$

It is clear from Eq. (2-21) that with $\beta = 0$, $\bar{\phi} = 0$. Furthermore, $\overline{\phi^2}$ is given by (Ref. 2-6)

$$\overline{\phi^2} = \int_{-\pi}^{\pi} \phi^2\,p(\phi)d\phi = \frac{\sinh\pi\beta}{\pi\,|\,I_{j\beta}(\alpha)\,|^2}\left\{\frac{I_0(\alpha)}{\beta}\left[\frac{\pi^2 I_0(\alpha)}{3} + 4\sum_{k=1}^{\infty}\frac{(-1)^k I_k(\alpha)}{k^2}\right] + 2\beta\,I_0(\alpha)\sum_{k=1}^{\infty}\frac{I_k(\alpha)}{k^2(\beta^2 + k^2)}\right.$$
$$\left. + 2\beta\sum_{k=1}^{\infty}\frac{(-1)^k I_k(\alpha)}{\beta^2 + k^2}\left[\left(\frac{\pi^2}{3} + \frac{1}{2k^2}\right)I_k(\alpha) + 4\sum_{\substack{m=1 \\ m\neq k}}^{\infty}\frac{(-1)^m(k^2 + m^2)\,I_m(\alpha)}{(k^2 - m^2)^2}\right]\right\} \tag{2-22}$$

The variance $\sigma_\phi^2 = \overline{\phi^2} - (\bar{\phi})^2$ is minimized when the loop is designed such that $\beta = 0$ and α is maximized (Ref. 2-6). For this case we have, from Eqs. (2-21) and (2-22),

$$\sigma_\phi^2 = \frac{\pi^2}{3} + \frac{4}{I_0(\alpha)} \sum_{k=1}^{\infty} \frac{(-1)^k}{k^2} I_k(\alpha) \qquad (2\text{-}23)$$

Finally, the expected value of the phase-error rate $\dot{\phi}$ is given by (Ref. 2-6)

$$\overline{\dot{\phi}} = \Omega_0 - AK\overline{\sin\phi} \qquad (2\text{-}24)$$

where $\overline{\sin\phi}$ is given in Eq. (2-20) with $n = 1$.

Figure 2-7 illustrates a plot of the variance of the phase-error σ_ϕ^2-reduced modulo 2π for various values of r with $\beta = 0$. For purposes of checking the validity of the approximation that leads to Eq. (2-18), we have plotted various values of variance of the phase-error obtained by direct measurement in the laboratory (Ref. 2-5). From Fig. 2-5 it is clear that for most practical purposes Eq. (2-18) characterizes the distribution $p(\phi)$ for all $\rho > 3$ dB when $r = 2$, $\beta \simeq 0$. The larger the value of r, the better is the approximation.

B. The Diffusion Coefficient

One method of accounting for the fact that the loop actually skips cycles is to evaluate the rate at which the actual process at work in the loop undergoes diffusion. This parameter, the so-called diffusion coefficient D (Ref. 2-6) is $(2\pi)^2$ times the total average number $\bar{S}$ of phase jumps (cycle slips) per unit of time and has been given by (Ref. 2-6)

$$D \triangleq \frac{4W_L r^2}{\rho(r+1)^2} \times \frac{\cosh \pi\beta}{|I_{j\beta}(\alpha)|^2} \triangleq (2\pi)^2 \bar{S} \qquad (2\text{-}25)$$

It will be shown later that the variance of the phase error $\tilde{\phi}(t)$ at time t starting from zero error at time $t = 0$ is

$$V \cong \overline{\phi^2} + Dt \qquad (2\text{-}26)$$

because the cross term $E[4\pi\,\phi(t)k(t)]$ is essentially zero. This condition of the cross term follows from the fact that $E[\phi(t)] \cong 0$ while $\tilde{\phi}(t)$ is essentially independent of $k(t)$. Here $k(t)$ is the unique integer with $\tilde{\phi}(t) = \phi(t) + 2\pi k(t)$.

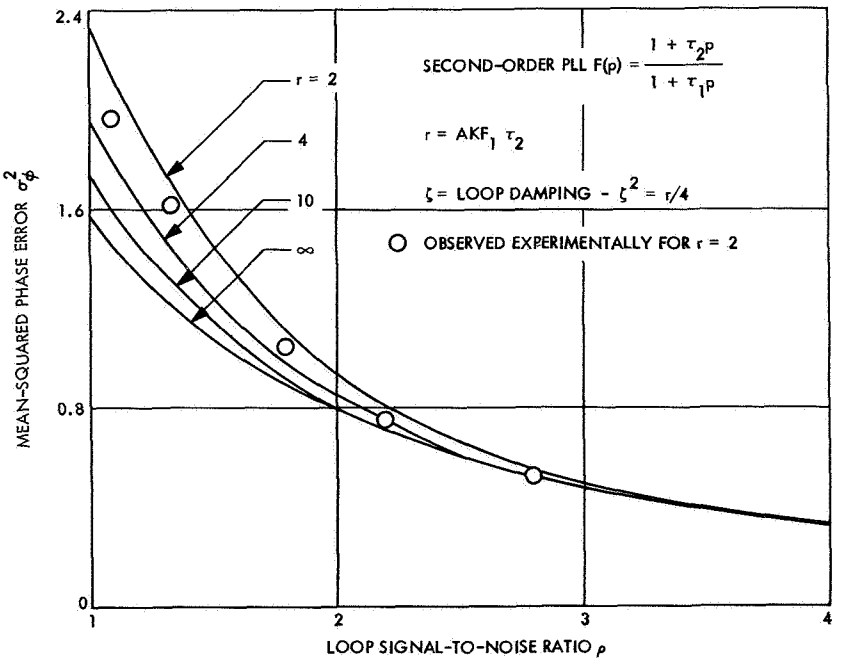

Fig. 2-7. Variance of the phase error vs loop signal-to-noise ratio ρ for various values of r, for $\rho > 3$ db, $\alpha \simeq \rho$

Figure 2-8 illustrates a plot of the normalized diffusion coefficient for various values of ρ and r with $\beta = 0$. From this figure it is seen that diffusion will not appreciably effect the measurement in a finite time if $\rho > 3$. Equations (2-21) and (2-25) can be used, via Eq. (2-26), to account for the effects of errors in doppler measurements produced by cycle slipping.

The expected time interval between successive phase jumps is approximated by (Ref. 2-6)

$$\Delta T \cong \frac{\pi^2 \rho(r+1)^2}{r^2 W_L} \times \frac{|\, I_{j\beta}(\alpha)\,|^2}{\cosh \pi\beta}$$

where it has been assumed that $\beta \ll 1$.

In the case where $\Omega_0 \neq 0$, the case of greatest practical interest, the average number of cycles slipped "to-the-right," say I_+, is of interest. Formulas for I_+ and I_- are given by (Ref. 2-6)

$$I_\pm \cong \frac{e^{\pm\beta\pi}\, I}{2 \sinh \pi\beta} \tag{2-27}$$

where I is the (net) average number of phase jumps per unit time, i.e.,

$$I = I_+ - I_- \cong \left[\frac{\rho(r+1)^2}{W_L(r\pi)^2}\right]^{-1} \times \frac{\sinh \pi\beta}{|\, I_{j\beta}(\alpha)\,|^2} \tag{2-28}$$

Now $I_+ = I_-$ for the unstressed loop with $\Omega_0 = 0$.

The quantity I is related to the total expected number of cycles slipped per unit time $\bar{S}$ through the equation

$$I \cong \left[\frac{\sinh \pi\beta}{\cosh \pi\beta}\right] \bar{S} \cong (\tanh \pi\beta)\bar{S} \tag{2-29}$$

C. Statistical Dynamics of the Phase-Error Process $\tilde{\phi}(t)$

The actual loop phase error $\tilde{\phi}(t)$ is related to the reduced modulo 2π process $\phi(t)$ through

$$\tilde{\phi}(t) = 2\pi k + \phi(t) \tag{2-30}$$

where

$$k = \left[\frac{\tilde{\phi}(t) - \phi(t)}{2\pi}\right] \tag{2-31}$$

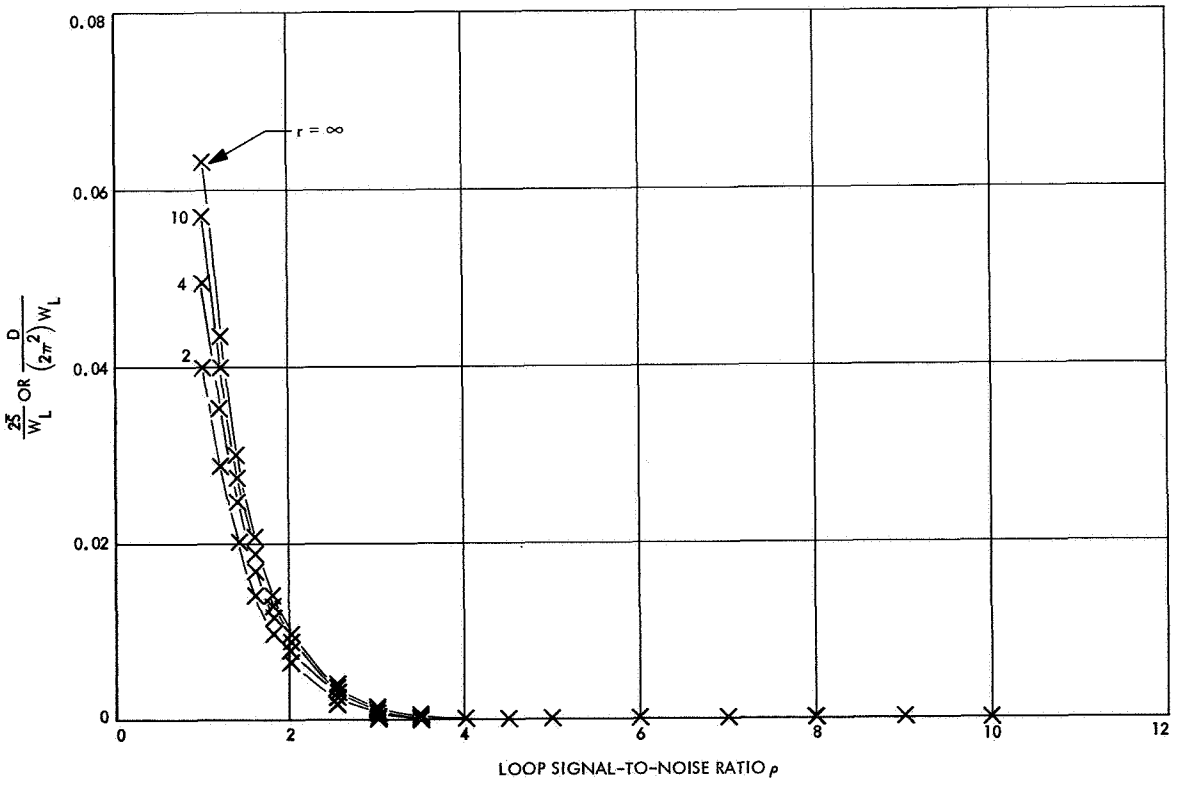

Fig. 2-8. The diffusion coefficient vs ρ for various values of r

is the largest integer that does not exceed the bracketed ratio. Thus, k is a discrete random variable that takes on integer values at random points in time. The mean squared value of the $\tilde{\phi}(t)$ process is given by

$$\sigma^2_{\tilde{\phi}}(t) = \sigma^2_{\phi}(t) + (2\pi)^2\sigma^2_k + 2\pi(\overline{k\phi} - \bar{k}\,\bar{\phi}) \quad (2\text{-}32)$$

Denote by $\mathcal{S}$ the event that k phase jumps occur in t seconds. If we assume that $\mathcal{S}$ is a Poisson-type process, then the quantity $\bar{S}$, representing the total average number of phase jumps per unit time can be used to produce a probabilistic model for the phase-jumping process that causes diffusion of the phase error process $\tilde{\phi}(t)$. Namely,

$$P(\mathcal{S}) \triangleq P(k) \cong \frac{(\bar{S}t)^k \exp(\bar{S}t)}{k!} \quad (2\text{-}33)$$

and the mean of k is

$$\bar{k} = \bar{S}t \quad (2\text{-}34)$$

with

$$\sigma^2_k = \bar{S}t \quad (2\text{-}35)$$

Experimental justification that supports the Poisson assumption is given in Refs. 2-7, 2-8, and 2-9. Thus the mean-squared value of $\tilde{\phi}(t)$ becomes

$$\sigma^2_{\tilde{\phi}}(t) = \sigma^2_{\phi}(t) + (2\pi)^2\,\bar{S}t + 2\pi(\overline{k\phi} - \bar{k}\,\bar{\phi}) \quad (2\text{-}36)$$

and, in the steady state, $\tilde{\phi}(t)$ has infinite variance. Now $D = (2\pi)^2\,\bar{S}$ represents the diffusion coefficient of the $\tilde{\phi}(t)$ process, i.e., the rate at which $\tilde{\phi}(t)$ is undergoing diffusion. Furthermore, if the random variables k and ϕ are independent, as is reasonable, we can write

$$\lim_{t\to\infty} \Delta\sigma^2_{\tilde{\phi}} = \sigma^2_{\tilde{\phi}}(t+T) - \sigma^2_{\tilde{\phi}}(t) = DT \quad (2\text{-}37)$$

Finally, the probability of losing phase lock in t seconds, i.e., the probability of slipping one or more cycles, is given by

$$P(\mathcal{S} \geq 1) \cong 1 - \exp(-\bar{S}t) \quad (2\text{-}38)$$

This result can be used in the design of phase-coherent doppler tracking systems; this topic is discussed more fully in Chapter 5.

References

2-1. Tausworthe, R. C., *Theory and Practical Design of Phase-Locked Receivers,* Technical Report 32-819. Jet Propulsion Laboratory, Pasadena, Calif., Feb. 15, 1966.

2-2. Tikhonov, V. I., "The Effect of Noise on Phase-Locked Oscillator Operation," *Automation and Remote Control,* Vol. 20, pp. 1160–1168, 1959. Translated from *Avtomatika i Telemekhaniki, Akademya Nauk SSSR,* Vol. 20, Sept. 1959.

2-3. Tikhonov, V. I., "Phase-Lock Automatic Frequency Control Operation in the Presence of Noise," *Automation and Remote Control,* Vol. 21, pp. 209-214, Mar. 1960. Translated from *Avtomatika i Telemekhaniki, Akademya Nauk SSSR,* Vol. 21, pp. 301–309, Mar. 1960.

2-4. Viterbi, A. J., "Phase-Locked Loop Dynamics in the Presence of Noise by Fokker–Planck Techniques," *Proceedings of the IEEE,* Vol. 57, pp. 1737–1753, Dec. 1963.

2-5. Charles, F. J., and Lindsey, W. C., "Some Analytical and Experimental Phase-Locked Loop Results for Low Signal-to-Noise Ratios," *Proceedings of the IEEE,* Vol. 51, pp. 1152–1166, Sept. 1966.

References (contd)

2-6. Lindsey, W. C., *Nonlinear Analysis and Synthesis of Generalized Tracking Systems, Parts I and II,* Technical Report USCEE 317 and 342. University of Southern California, Los Angeles, Calif., Dec. 1968.

2-7. Charles, F. J., and Lindsey, W. C., "Some Analytical and Experimental Phase-Locked Loop Results for Low Signal-to-Noise Ratios," *Proceedings of the IEEE,* Vol. 55, No. 9, pp. 1152–1166, Sept. 1966.

2-8. Tausworthe, R. C., and Sanger, D., "Experimental Study of the First-Slip Statistics of the Second-Order Phase-Locked Loop," in *Supporting Research and Advanced Development,* Space Programs Summary 37-43, Vol. III, pp. 76–80, Jet Propulsion Laboratory, Pasadena, Calif., 1967.

2-9. Sanneman, R. W., and Rowbotham, J. R., "Random Characteristics of the Type II Phase-Locked Loop," *IEEE Transactions on Aerospace and Electronic Systems,* Vol. AES-3, No. 4, July 1967.

Chapter 3
The Second-Order Phase-Locked Loop Preceded by a Band-Pass Limiter

The theoretical results needed to explain the behavior of the carrier-tracking loop (PLL) when preceded by a BPL are discussed. The detailed theory and operation of the BPL is covered more completely in Refs. 3-1, 3-2, and 3-3.

I. The Linear PLL Theory and the Effects of Band-Pass Limiting

In the practical operation of a coherent receiving system employing PLLs, the loop is preceded by a BPL because the loop bandwidth is a function of the signal power P, and any fluctuation in P (owing to a change in range, for instance) causes the loop bandwidth to fluctuate similarly. Band-pass limiters are used also to protect various loop components, the multiplier in particular, where signal and noise levels can vary over several orders of magnitude and exceed the dynamic range of these components. The mechanization of a BPL is illustrated in Fig. 3-1; the limiter incorporated in the PLL system is shown in Fig. 3-2.

Again, the variance of the phase error is an important parameter in specifying the loop response to a sine wave plus noise. If the spectral density of the noise at the limiter output is denoted by $S_l(s)$, and the bandwidth of the loop is assumed small in comparison with the bandwidth of the spectrum of the limiter output, one may derive a result similar to Eq. (2-9), viz.,

$$\sigma^2 = \frac{S_l(0)W_L}{\alpha_l^2} \tag{3-1}$$

where α_l^2 is the power of the signal component of the limiter output and $1 - \alpha_l^2$ is the power associated with the noise process at the limiter output. The limiter output spectrum has some noise bandwidth, say

$$w_l = \frac{1}{S_l(0)}\left[\frac{1}{2\pi j}\int_{-j\infty}^{j\infty} S_l(s)\,ds\right] = \frac{1-\alpha_l^2}{S_l(0)} \tag{3-2}$$

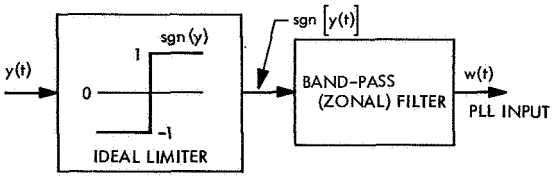

Fig. 3-1. Mechanization of a BPL

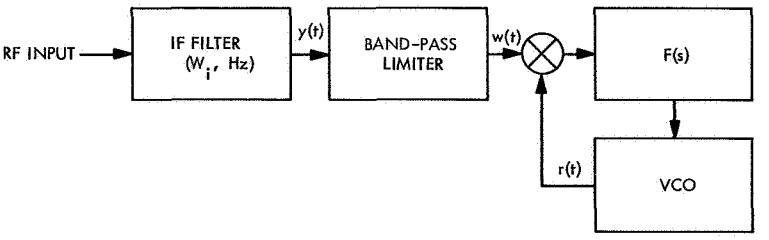

$y(t) = \sqrt{2P}\ \sin\ [\omega t + \theta]$ + WHITE NOISE (SINGLE-SIDED SPECTRAL DENSITY N_0 W/Hz)

$w(t) = \sqrt{2\alpha_\ell}\ \sin\ [\omega t + \theta]$ + NOISE

$r(t) = \sqrt{2}\ \cos\ [\omega t + \hat{\theta}]$

Fig. 3-2. PLL receiver preceded by a BPL

since the integral represents the total output noise power in the zone of interest, and the variable s is the Laplace transform operator. Thus, as a result,

$$\sigma^2 = \frac{1 - \alpha_\ell^2}{\alpha_\ell^2}\left(\frac{W_L}{w_\ell}\right) = \frac{W_L}{\rho_\ell w_\ell} \tag{3-3}$$

where ρ_ℓ is the output signal-to-noise ratio of the limiter. In practice, α_ℓ is usually referred to as the signal amplitude suppression factor, and is given by (Ref. 3-2)

$$\alpha_\ell = \sqrt{\frac{\pi}{2}}\left(\frac{\eta_\ell}{2}\right)^{1/2} \exp\left(-\frac{\eta_\ell}{2}\right)\left[I_0\left(\frac{\eta_\ell}{2}\right) + I_1\left(\frac{\eta_\ell}{2}\right)\right] \tag{3-4}$$

where $I_k(z)$ is the modified Bessel function of argument z and order k and $\eta_\ell = 2P/N_0W_i$ is the signal-to-noise ratio input to the limiter. The parameter W_i is used to denote the bandwidth of the IF filter. In the region of interest in practice Eq. (3-4) is closely approximated by (Ref. 3-1)

$$\alpha_\ell^2 = \frac{0.7854\,xy + 0.4768\,x^2y^2}{1 + 1.024\,xy + 0.4768\,x^2y^2} = \frac{0.7854\,\eta + 0.4768\,\eta^2}{1 + 1.024\,\eta + 0.4768\,\eta^2} \tag{3-5}$$

where

$$\eta = xy \tag{3-6}$$

and

$$x = \frac{2P}{N_0W_L}; \qquad y = \frac{W_L}{W_i} \tag{3-7}$$

The parameter x is, of course, the signal-to-noise ratio existing in the bandwidth of the loop. Thus, Eq. (3-3) may be written as

$$\sigma^2 = \frac{W_L}{\rho_\ell w_\ell} \times \frac{\eta_\ell}{\eta_\ell} = \frac{N_0W_L}{2P} \times \frac{W_i}{w_\ell} \times \frac{\eta_\ell}{\rho_\ell} = \frac{N_0W_L}{2P}\,\Gamma \tag{3-8}$$

where W_L is to be subsequently defined. The factor $\Gamma = W_i\eta_\ell/w_\ell\,\rho_\ell$ is the limiter performance factor (p. 48 of Ref. 3-1) that is well approximated in the region of practical interest by

$$\Gamma = \frac{1 + 0.345\,xy}{0.862 + 0.690\,xy} \tag{3-9}$$

where x and y are defined by Eq. (3-7). Finally, α_ℓ^2 takes the place of P given in Chapter 2; therefore, preceding the loop by a BPL greatly complicates the analysis even in the linear case. However, it is convenient to build a working theory based upon simplifying assumptions, and to test the validity of this theory through experimentation in the laboratory.

Thus, the transfer function for a PLL preceded by a BPL [from Eq. (2-8)] is

$$H(p) = \frac{1 + \tau_2 p}{1 + \left(\tau_2 + \frac{1}{\alpha_\ell K}\right)p + \left(\frac{\tau_1}{\alpha_\ell K}\right)p^2} \tag{3-10}$$

and the corresponding W_L becomes

$$W_L = \frac{1 + \frac{\alpha_\ell K\tau_2^2}{\tau_1}}{2\tau_2\left(1 + \frac{1}{\alpha_\ell K\tau_2}\right)} = \frac{1 + r}{2\tau_2\left(1 + \frac{\tau_2}{r\tau_1}\right)} \tag{3-11}$$

where

$$r \triangleq \frac{\alpha_l K \tau_2^2}{\tau_1} \tag{3-12}$$

Notice that W_L is now a function of the limiter suppression factor α_l.

II. The Nonlinear PLL Theory and the Effects of Band-Pass Limiting

As a rule, PLL parameters are usually specified at what shall be referred to as the "design point." The "design point" is frequently referred to as "loop threshold." In the past, this point has been taken to imply that condition where[1]

$$2P_0 = N_0 W_{L0} \tag{3-13}$$

and

$$W_{L0} = \frac{1 + r_0}{2\tau_2\left(1 + \frac{\tau_2}{r_0\tau_1}\right)}, \qquad r_0 = \frac{\alpha_{l0} K \tau_2^2}{\tau_1}$$

The subscript zero on P, W_L, and r refers to the respective values of these parameters at the "design point." It is known (Ref. 3-1) that P_0 represents a signal power at which the linear PLL theory does not apply.

What theory, then, may be used to predicate a particular design, or to test the performance of a particular design? In the following discussion, an approximate model is presented together with experimental results that verify it.

The distribution of the phase error for a second-order PLL is, for all practical purposes, characterized by the parameter α defined by Eq. (2-15). In the linear model, α is the reciprocal of the variance of the phase error. This suggests that the distribution of the phase error in a loop that is preceded by a limiter be characterized by the assumption that α is the reciprocal of the variance of the phase error as determined from the linear PLL theory when preceded by a limiter; i.e.,

$$\alpha = \frac{2P}{N_0 W_L \Gamma} \tag{3-14}$$

[1]Where limiters are present in the results that follow, Eq. (3-13) is assumed always true. This applies as well in all the figures that follow. It is also assumed that $\beta \simeq 0$ and that $\alpha \simeq \rho$ in Eq. (2-19).

Thus, the distribution of the phase error in a PLL preceded by a limiter is approximated by

$$p(\phi) = \frac{\exp(\alpha \cos\phi)}{2\pi I_0(\alpha)} = \frac{\exp\left[\left(\frac{2P}{N_0 W_L \Gamma}\right)\cos\phi\right]}{2\pi I_0\left(\frac{2P}{N_0 W_L \Gamma}\right)}, \qquad |\phi| \le \pi \tag{3-15}$$

where Γ is defined in Eq. (3-9). Because W_L is a function of α_l, this dependence must be determined before any attempt to use Eq. (3-15).

At the "design point," the loop bandwidth and signal suppression factor are denoted by W_{L0} and α_{l0}, respectively. For values that differ from the "design-point" value, W_L and α_l are used. Thus the transfer function of the loop becomes

$$H(s) = \frac{1 + \left(\frac{r_0 + 1}{2W_{L0}}\right)s}{1 + \left(\frac{r_0 + 1}{2W_{L0}}\right)s + \frac{\mu}{r_0}\left(\frac{r_0 + 1}{2W_{L0}}\right)^2 s^2} \tag{3-16}$$

where

$$\mu = \frac{\alpha_{l0}}{\alpha_l} \tag{3-17}$$

The parameter μ will be referred to as the limiter suppression factor. Hence

$$W_L = \frac{1}{2\pi j}\int_{-j\infty}^{j\infty} |H(s)|^2\, ds = W_{L0}\left(\frac{1 + \frac{r_0}{\mu}}{1 + r_0}\right) \tag{3-18}$$

and the variance of the phase error becomes

$$\sigma^2 = \int_{-\pi}^{\pi} \phi^2 p(\phi)\, d\phi = \frac{\pi^2}{3} + \frac{4}{I_0(\alpha)}\sum_{k=1}^{\infty}\frac{(-1)^k I_k(\alpha)}{k^2} \tag{3-19}$$

where

$$\alpha = \frac{2P}{N_0 W_{L0}} \times \left(\frac{1}{\Gamma}\right)\left(\frac{1 + r_0}{1 + \frac{r_0}{\mu}}\right) \tag{3-20}$$

and Γ, r_0, and μ are defined by Eqs. (3-9), (3-12), and (3-17). respectively. The functions $I_k(x)$ in Eq. (3-19) are imaginary Bessel functions.

Figure 3-3 is a plot of Eq. (3-19) for various values of y. This figure plots the variance of the phase-error σ^2 vs the signal-to-noise ratio x existing in the "design-point" loop bandwidth as determined from the linear PLL theory. The variance is essentially independent of the parameter y; the parameter $y = W_{Lo}/W_i$ is the ratio of the "design-point" loop bandwidth to the bandwidth of the filter (IF amplifier) preceding the BPL of Fig. 3-1. Figure 3-4 is plotted under the same conditions as Fig. 3-3, except that the nonlinear PLL theory is assumed. Comparison of Fig. 3-3 with Fig. 3-4 indicates the difference between the variances of phase error determined from the linear PLL theory and the nonlinear PLL theory where the loops are preceded by a BPL. Note that the variance of the phase error in both plots is relatively insensitive to y.

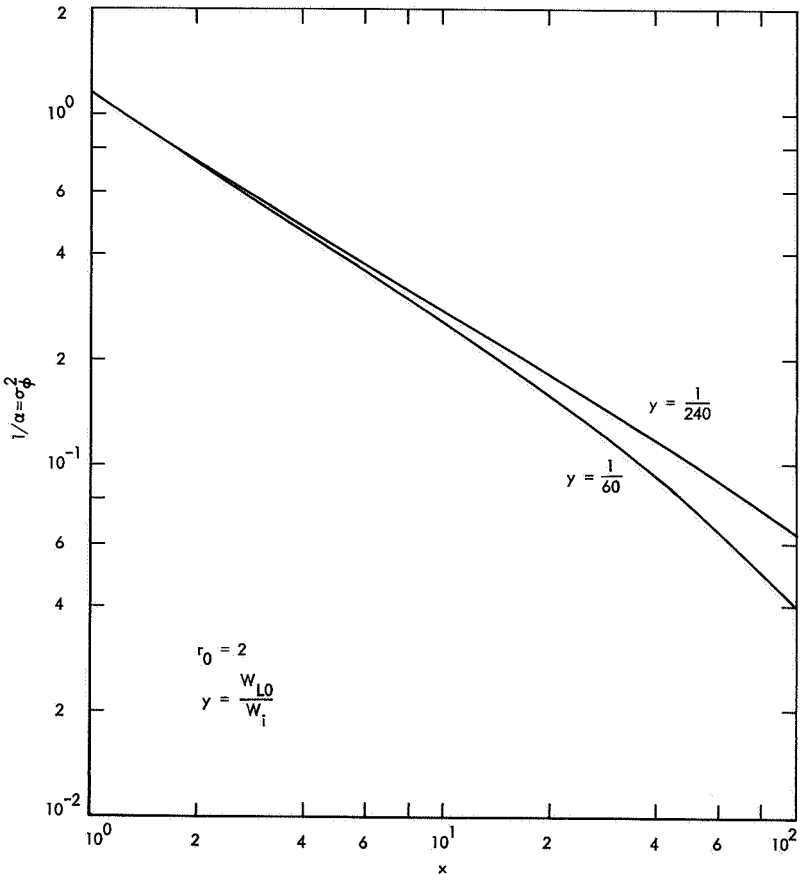

Fig. 3-3. Variance of the phase error σ_ϕ^2 vs the signal-to-noise ratio x; linear PLL theory is assumed with BPLs preceding the loop

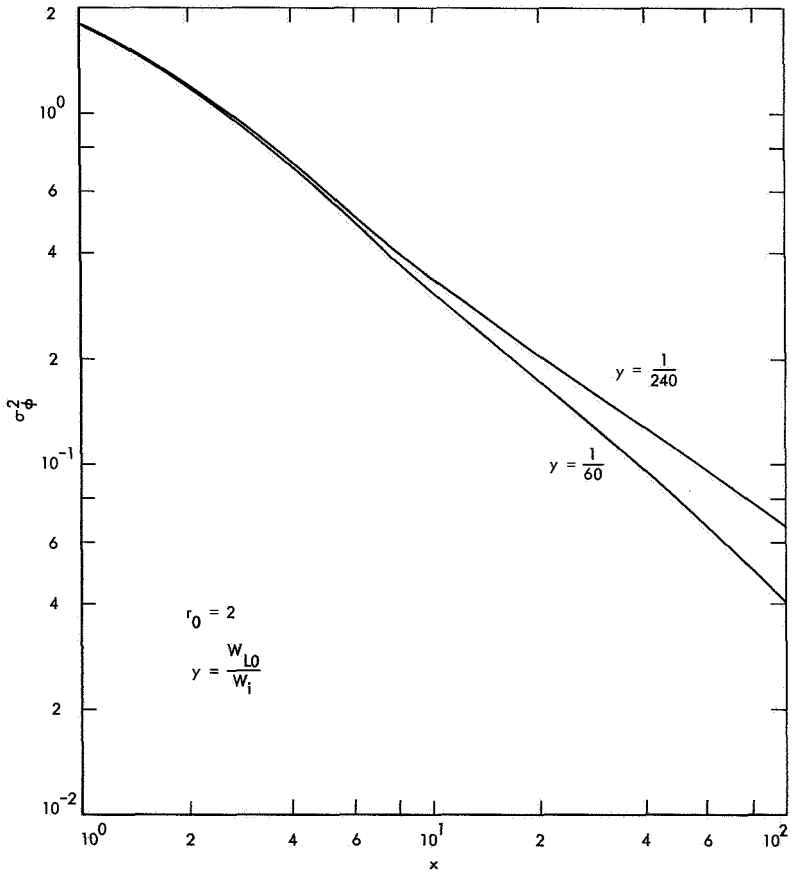

Fig. 3-4. Variance of the phase error σ^2_ϕ vs the signal-to-noise ratio x; nonlinear PLL theory is assumed with BPLs preceding the loop

References

3-1. Tausworthe, R. C., *Theory and Practical Design of Phase-Locked Receivers: Volume I.* Technical Report 32-819. Jet Propulsion Laboratory, Pasadena, Calif., Feb. 15, 1966.

3-2. Davenport, W. B., "Signal-to-Noise Ratios in Band-Pass Limiters," *Journal of Applied Physics,* Vol. 24, No. 6, pp. 720-727, June 1953.

3-3. Springett, J. C., "Signal-to-Noise and Signal-to-Noise Spectral-Density Ratios at the Output of a Filter-Limiter Combination," in *Supporting Research and Advanced Development,* Space Programs Summary 37-36, Vol. IV, Dec. 31, 1965.

Chapter 4

Radio-Frequency Phase Measurements in One-Way and Two-Way Phase-Coherent Communication Systems

In a phase-coherent communication system for deep-space applications, the telemetry and command signals usually phase modulate the radio-frequency carrier with modulation indices sufficiently low to permit the spectrum of the transmitted waveform to retain a portion of the total transmitter power at the carrier frequency. There are two reasons for this. First, the velocity of the vehicle must be measured. This is usually accomplished by measuring the apparent doppler shift at the reference system and thereby computing the velocity. This measurement will be discussed in detail in Chapter 5. Second, if the telemetry and command data are to be detected coherently, the measurement or estimation of the phase of the observed carrier in noise is essential. The problem of phase measurement or phase estimation is the subject of this chapter. The theory developed in what follows either includes or excludes the effects of BPLs in both the vehicle and the reference systems as well as the effects on system design due to the nonlinear behavior of PLLs.

I. Basic System Model

Figure 4-1 shows the simplest mechanization of the two-way phase-measuring system. The reference system emits, on the uplink, the waveform

$$\rho(t) = \sqrt{2P_{c1}} \sin \omega_0 t \tag{4-1}$$

After transmission, the channel introduces an arbitrary and unknown phase shift θ_1 in the transmitted waveform, and further disturbs $\rho(t)$ with additive white Gaussian noise $n_1(t)$ of single-sided spectral density N_{10} W/Hz. We observe in the vehicle the doppler-shifted, phase-shifted, noise-corrupted waveform

$$\psi(t) = \sqrt{2P_{c1}} \sin (\omega_1 t + \theta_1) + n_1(t) \tag{4-2}$$

The additive noise process $n_1(t)$ may be represented by

$$n_1(t) = x_1(t) \cos (\omega_1 t + \theta_1) + y_1(t) \sin (\omega_1 t + \theta_1) \tag{4-3}$$

where $x_1(t)$ and $y_1(t)$ are statistically independent, stationary white Gaussian noise processes of single-sided spectral density N_{10}. The vehicle coherently tracks, by means of a narrow-band PLL, the carrier that produces the estimate

$$z(t) = \sqrt{2} \cos (\omega_1 t + \hat{\theta}_1) \tag{4-4}$$

where $\hat{\theta}_1$ is the PLL estimate of θ_1.

The source of the carrier for the downlink in a two-way phase-measuring system is derived from the vehicle's carrier-tracking loop. Thus, on the downlink, we transmit

$$\eta(t) = \sqrt{2P_{c2}} \sin (\omega_{10} t + \hat{\theta}_1) \tag{4-5}$$

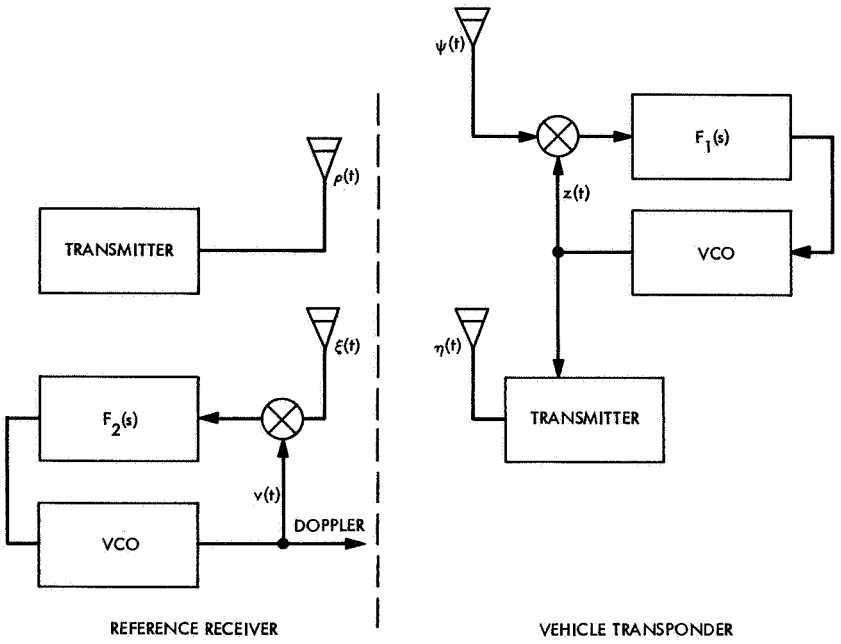

Fig. 4-1. Simplest two-way phase-measuring system

and observe, at the reference system, the doppler-shifted, phase-shifted, noise-corrupted waveform

$$\xi(t) = \sqrt{2P_{c2}} \sin(\omega_2 t + \hat{\theta}_1 + \theta_2) + n_2(t) \qquad (4\text{-}6)$$

where $n_2(t)$ is stationary white Gaussian noise of single-sided spectral density N_{20} W/Hz, and $\omega_{10} = G\omega_1$ [Eq. (4-5)], where G denotes the static phase gain of the vehicle transponder. A convenient representation for $n_2(t)$ is given by

$$n_2(t) = x_2(t) \cos(\omega_2 t + \hat{\theta}_1 + \theta_2) + y_2(t) \sin(\omega_2 t + \hat{\theta}_1 + \theta_2) \qquad (4\text{-}7)$$

where $x_2(t)$ and $y_2(t)$ are statistically independent and white Gaussian noise processes of single-sided spectral density N_{20} W/Hz. The reference receiver tracks the carrier component in $\xi(t)$, which provides the receiver with the estimate

$$v(t) = \sqrt{2} \cos(\omega_2 t + \hat{\theta}_2) \qquad (4\text{-}8)$$

The quantity $\hat{\theta}_2$ is the PLL estimate of $\hat{\theta}_1 + \theta_2$.

In the design of such a system, there are at least two errors that are significant. These are: (1) the reference receiver's two-way-tracking phase error $\phi_{r2} = \hat{\theta}_1 + \theta_2 - \hat{\theta}_2$, and (2) the two-way-doppler phase error $\phi_{d2} = \hat{\theta}_2 - \theta_0$, where θ_0 is the phase of the transmitted carrier (assumed here to be zero). In the next section, the phase error ϕ_{r2} and its relationship to system parameters employing the linear PLL theory will be considered; in Section III, the problem will be remodeled to permit consideration of the nonlinear effects of the PLL. Finally, the phase error when BPLs precede the vehicle- and reference-system PLLs will be studied in Section IV.

II. Two-Way-Tracking Phase Error (Linear PLL Theory)

In linearized form, the important features of the system in Fig. 4-1 are illustrated in Fig. 4-2. (In these figures, s denotes the Laplace transform variable.) The parameter G is determined by the ratio of the output carrier frequency. The filter functions $H_n(s)$, where $n = 1, 2$, are the closed-loop transfer functions of the system's carrier-tracking loops. The parameter $n = 1$ corresponds to elements located in the vehicle subsystem, while $n = 2$ corresponds to elements located in the reference system.

To specify the mathematical form of $H_n(s)$, the form of the loop filters $F_n(s)$, where $n = 1, 2$, in Fig. 4-1 must be specified. As indicated in Chapter 2, the loop filter that corresponds to the one generally employed for

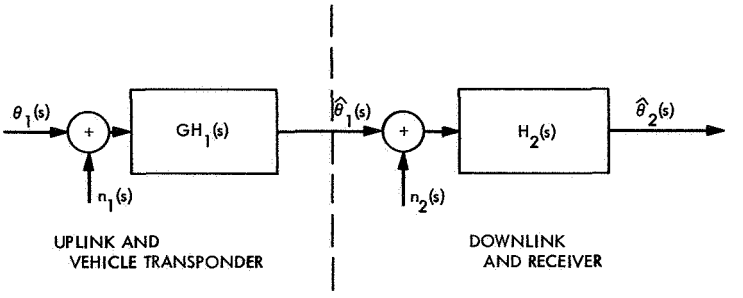

Fig. 4-2. Linearized two-way-doppler and phase-measuring system

carrier-tracking purposes is of the proportional-plus-integral control type, viz,

$$F_n(s) = \frac{1 + \tau_{2n}s}{1 + \tau_{1n}s}, \qquad n = 1, 2 \tag{4-9}$$

and the corresponding $H_n(s)$ is determined from Eq. (2-6), viz.,

$$H_n(s) = \frac{1 + \tau_{2n}s}{1 + \left(\tau_{2n} + \dfrac{1}{K_n\sqrt{P_{cn}}}\right)s + \left(\dfrac{\tau_{1n}}{K_n\sqrt{P_{cn}}}\right)s^2} \tag{4-10}$$

As before, it is convenient to define the quantity r_n as

$$r_n = \frac{K_n\tau_{2n}^2\sqrt{P_{cn}}}{\tau_{1n}} \tag{4-11}$$

and the loop bandwidth W_{Ln} as

$$W_{Ln} = \frac{1}{2\pi j}\int_{-j\infty}^{j\infty} |\, H_n(s)\,|^2\, ds, \qquad n = 1, 2 \tag{4-12}$$

Substituting Eq. (4-10) into Eq. (4-12) and carrying out the integration, we have

$$W_{Ln} = \frac{1 + r_n}{2\tau_{2n}\left(1 + \dfrac{\tau_{2n}}{r_n\,\tau_{1n}}\right)} \approx \frac{1 + r_n}{2\tau_{2n}} \tag{4-13}$$

the latter approximation being valid when $r_n\tau_{1n} \gg \tau_{2n}$. Thus, the use of Eq. (4-13) in Eq. (4-10) leads to the most useful form of $H_n(s)$, viz.,

$$H_n(s) = \frac{1 + \left(\dfrac{r_n + 1}{2W_{Ln}}\right)s}{1 + \left(\dfrac{r_n + 1}{2W_{Ln}}\right)s + \dfrac{1}{r_n}\left(\dfrac{r_n + 1}{2W_{Ln}}\right)^2 s^2}, \qquad n = 1, 2 \tag{4-14}$$

From Eq. (4-10) one may derive the system-damping behavior. For $r_n < 4$, the roots of the denominator polynomial lead to an underdamped system, with damping factor ζ and loop natural frequency Ω_{n0} given by

$$\zeta_n = \frac{1}{2}\left(1 + \frac{\tau_{2n}}{r_n}\right)\sqrt{r_n} \sim \frac{\sqrt{r_n}}{2}$$

$$\Omega_{n0} = \frac{K_n\sqrt{P_{cn}}}{\tau_{1n}} = \frac{\sqrt{r_n}}{\tau_{2n}} \tag{4-15}$$

For $r_n = 4$, critical damping ($\zeta_n = 1$) occurs and, for $r_n \gg 4$, $H_n(s)$ has two real negative poles.

The reference receiver's tracking phase error ϕ_{r2} is defined as the difference between the receiver output phase and the receiver input phase,

$$\phi_{r2}(s) = \theta_2 + \hat{\theta}_1(s) - \hat{\theta}_2(s) \tag{4-16}$$

We note that the noise that enters the vehicle transponder must be considered as part of the reference receiver's input signal $\hat{\theta}_1(s) + \theta_2$. Thus, the Laplace transform of the phase error $\phi_{r2}(s)$ is

$$\phi_{r2}(s) = n_1(s)GH_1(s)[1 - H_2(s)] + n_2(s)H_2(s) \tag{4-17}$$

and the mean-squared value of the reference receiver's tracking phase error is

$$\sigma^2_{\phi_{r2}} = \frac{1}{2\pi j}\int_{-j\infty}^{j\infty} \phi_{r2}(s)\,\phi_{r2}(-s)\,ds \qquad (4\text{-}18)$$

which becomes (using linear PLL theory)

$$\sigma^2_{\phi_{r2}} = \frac{1}{2\pi j}\left[\frac{N_{10}G^2}{2P_{c1}}\int_{-j\infty}^{j\infty} |\,H_1(s)\,|^2\,|\,1 - H_2(s)\,|^2\,ds + \frac{N_{20}}{2P_{c2}}\int_{-j\infty}^{j\infty} |\,H_2(s)\,|^2\,ds\right] \qquad (4\text{-}19)$$

Substituting Eq. (4-14) into Eq. (4-19) and integrating the result, we have

$$\sigma^2_{\phi_{r2}} = \frac{1}{\alpha_1} + \frac{1}{\alpha_2} \qquad (4\text{-}20)$$

where

$$\alpha_1 = \frac{2P_{c1}}{W_{L1}N_{10}} \times \frac{1}{G^2K_R(r_1, r_2, \beta)}$$

$$\alpha_2 = \frac{2P_{c2}}{N_{20}W_{L2}}$$

and

$$K_R(r_1, r_2, \beta) = \frac{r_1\beta}{r_2(r_1+1)} \times \left[\frac{r_2 + r_1r_2\beta(1+\beta) + \beta^2(1+\beta) + r_1\beta^3}{\frac{r_2}{r_1} + r_2\beta + \beta^2(r_1 + r_2 - 2) + r_1\beta^3 + \frac{r_1\beta^4}{r_2}}\right]$$

$$\beta = \frac{W_{L1}(r_2+1)}{W_{L2}(r_1+1)}$$

The function $K_R(r_1, r_2, \beta)$ has been computed and the results are plotted in Fig. 4-3 for various values of $r_1 = r_2 = r$ and β. In this figure, $\beta = W_{L1}/W_{L2}$, and no limiters are present in this system. It is evident from this figure that the parameters r_1, r_2, and β are significant in the design of two-way phase-measuring systems.

A comparison of the performance of a linear system that makes a two-way phase measurement (i.e., the signal

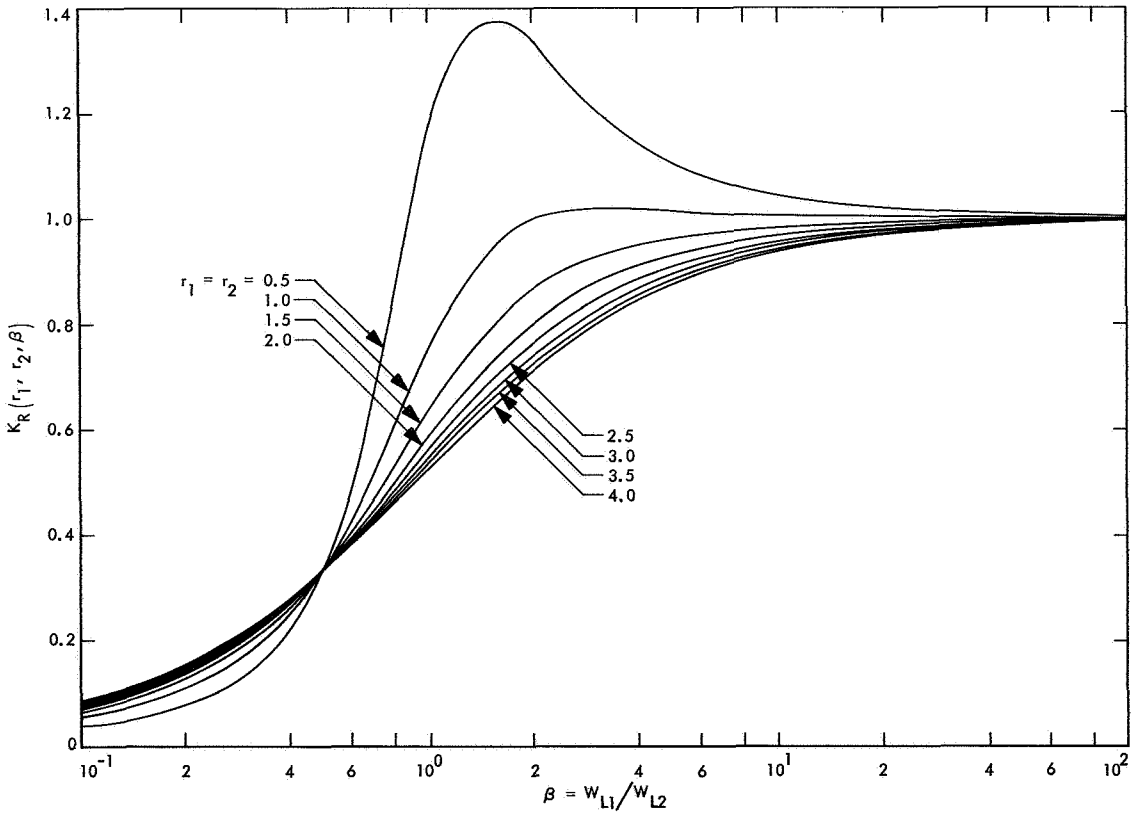

Fig. 4-3. The function $K_R(r_1, r_2, \beta)$ vs β for various values of system damping

relayed to the reference system is derived from a free-running oscillator on board the vehicle) with a linear system that makes a one-way measurement would be helpful. In the linear system, the reference receiver's phase error becomes $\sigma^2_{\phi_{r2}} = 1$. In a one-way linear system, this corresponds to the condition

$$\sigma^2_{\phi_{r1}} = \frac{2P'_{c2}}{N'_{20} W_{L2}} = 1 \tag{4-21}$$

and, because the noise in both cases is the same and the bandwidth of the reference receiver is $W'_{L2} = W_{L2}$, we have

$$N_{20} = \frac{2P'_{c2}}{W_{L2}} \tag{4-22}$$

which means

$$\sigma^2_{\phi_{r2}} = 1 = \left[\frac{2P_{c1}}{W_{L1}N_{10}} \times \frac{1}{G^2K_R(r_1, r_2, \beta)}\right]^{-1} + \left(\frac{P_{c2}}{P'_{c2}}\right)^{-1} \tag{4-23}$$

The ratio P_{c2}/P'_{c2} is the ratio of signal power in a two-way system to the signal power in a one-way system that produces a mean-square phase error of one radian:

$$\frac{P_{c2}}{P'_{c2}} = \frac{1}{1 - \dfrac{W_{L1}N_{10}}{2P_{c1}} G^2K_R(r_1, r_2, \beta)} \tag{4-24}$$

The parameter $2P_{c1}/W_{L1}N_{10}$ is the signal-to-noise ratio in the bandwidth of the vehicle's carrier-tracking loop x, as plotted in Fig. 4-4 against the ratio P_{c2}/P'_{c2}. Various values of the parameter $\beta = W_{L1}/W_{L2}$ are used in the figure; the linear PLL theory is assumed, and no limiters are present in the system.

III. Two-Way-Tracking Phase Error (Nonlinear PLL Theory)

Because the exact nonlinear PLL theory that pertains to the two-way phase measurement appears formidable, an approximate model for the probability distribution of the two-way phase error ϕ_{r2} may be developed on the basis of the PLL measurements presented in Chapter 2.

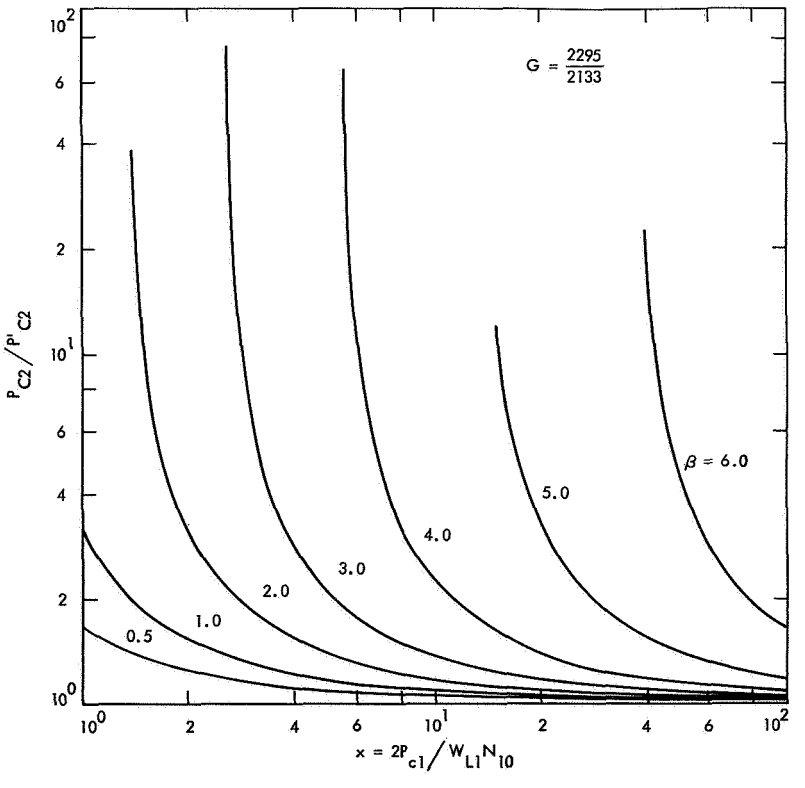

Fig. 4-4. Degradation in ground receiver sensitivity P_{c2}/P'_{c2} vs the signal-to-noise ratio x in the vehicle's carrier-tracking loop

The validity of this model's predictions of the exact performance of a two-way phase-measuring system must be checked by results obtained in the laboratory. Unfortunately, these measurements for the two-way system have not been made at present; the approximate distribution of the phase error, however, can be checked at the extremes of high and low signal-to-noise ratios.

For the present, the system phase error is denoted by $\phi_{r2} = \phi_2$. Then, on the basis of the results in Chapter 2, Section III, it is possible to show (Ref. 4-1) that the distribution of the two-way phase error is approximated by

$$p(\phi_2) = \frac{I_0(|\alpha_1 + \alpha_2 \exp(j\phi_2)|)}{2\pi I_0(\alpha_1) I_0(\alpha_2)}, \qquad |\phi_2| \leq \pi \tag{4-25}$$

where $I_0(x)$ is the imaginary Bessel function of zero order and of argument x, and α_1 and α_2 are defined in Eq. (4-20). This model distribution is valid only if G is approximately equal to unity; in practice, this is the case of greatest interest. The validity of using this distribution as a model for the distribution of the two-way phase error may be checked by considering the limiting cases of high and low signal-to-noise ratios. For large signal-to-noise ratios in the uplink and downlink carrier-tracking loops, the distribution [Eq. (4-25)] is Gaussian with zero mean and a variance of $\alpha_1^{-1} + \alpha_2^{-1}$; i.e.,

$$p(\phi_2) = \frac{\exp\left\{-\left[\dfrac{\phi_2^2}{2(\alpha_1^{-1} + \alpha_2^{-1})}\right]\right\}}{[2\pi(\alpha_1^{-1} + \alpha_2^{-1})]^{1/2}} \tag{4-26}$$

Thus, the distribution checks with the linear PLL theory for large signal-to-noise ratios. As α_1 and α_2 approach infinity,

$$\lim_{\alpha_1, \alpha_2 \to \infty} p(\phi_2) = \delta(\phi_2) \tag{4-27}$$

which means that perfect phase measurement is obtained.

For weak-signal conditions on either the uplink or the downlink, or both, Eq. (4-25) becomes uniformly distributed; i.e.,

$$\lim_{\alpha_1 \text{ or } \alpha_2 \to 0} p(\phi_2) = \frac{1}{2\pi}, \qquad |\phi_2| < \pi \tag{4-28}$$

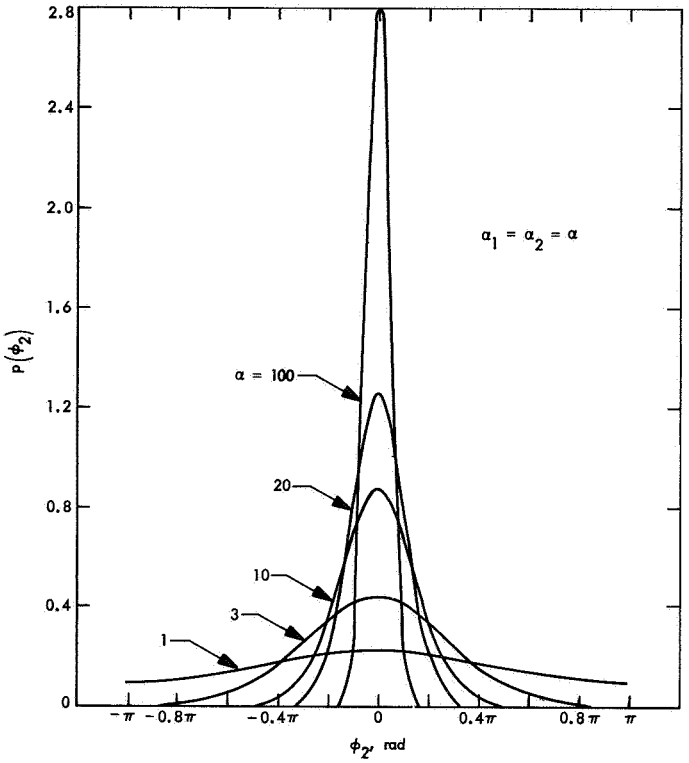

Fig. 4-5. Probability distribution $p(\phi_2)$ of the two-way phase error vs ϕ_2

This is in direct agreement with one's intuition for weak-signal strengths. Plotted in Fig. 4-5 is Eq. (4-25) for various values of $\alpha_1 = \alpha_2 = \alpha$.

The variance of this distribution is important in practice; i.e.,

$$\sigma_{\phi_2}^2 = \int_{-\pi}^{\pi} \phi_2^2 \, p(\phi_2) \, d\phi_2 = \sigma_{r2}^2 \tag{4-29}$$

Substitution of Eq. (4-25) into Eq. (4-29) leads to

$$\sigma_{r2}^2 = \sigma_{\phi_2}^2 = \frac{\pi^2}{3} + 4 \sum_{k=1}^{\infty} \frac{(-1)^k I_k(\alpha_1) I_k(\alpha_2)}{k^2 I_0(\alpha_1) I_0(\alpha_2)} \tag{4-30}$$

To illustrate, the general behavior of this variance [Eq. (4-30)] is plotted in Fig. 4-6 for various values of $\alpha_1 = \alpha_2 = \alpha$. For comparison purposes, results from the linear and nonlinear PLL theory of one-way links are shown (i.e., $n = 1$); no limiters are present in the system illustrated.

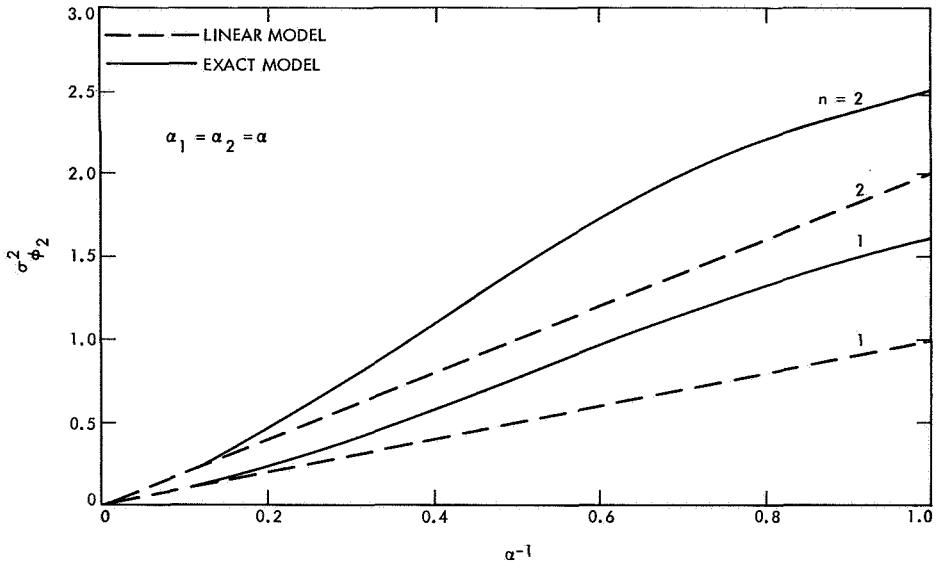

Fig. 4-6. Variance of the two-way phase error $\sigma^2_{\phi 2}$ ($n = 2$) vs the noise-to-signal ratio

IV. Two-Way-Tracking Phase Error Where the Carrier-Tracking Loops Are Preceded by BPLs (Linear PLL Theory)

In practice, and for the reasons given in Chapter 3, Section I, BPLs always precede the carrier-tracking loops. Figure 4-7 illustrates a typical mechanization of a practical two-way phase-measuring system.

Employing the linear PLL theory given in Chapter 3 [i.e., substituting Eq. (3-16) into Eq. (4-19)], we can easily show that the variance of the two-way phase measurement is given by

$$\sigma^2_{\phi_{r2}} = \sigma^2_{\phi_2} = \frac{1}{\alpha_{1l}} + \frac{1}{\alpha_{2l}} \tag{4-31}$$

where

$$\left.\begin{aligned} \alpha_{1l} &= \frac{2P_{c1}}{W_{10}N_{10}} \times \frac{1}{G^2\Gamma_1 K_R(k_1, k_2, \beta)} \\ \alpha_{2l} &= \frac{2P_{c2}}{N_{20}W_{20}} \left(\frac{1 + r_{20}}{1 + \frac{r_{20}}{\mu_2}}\right) \frac{1}{\Gamma_2} \end{aligned}\right\} \tag{4-32}$$

and Γ_n, $n = 1, 2$, are the limiter performance factors given by

$$\left.\begin{aligned} \Gamma_n &= \frac{1 + 0.345\, x_n y_n}{0.862 + 0.690\, x_n y_n} \\ x_n &= \frac{2P_{cn}}{N_{n0}W_{n0}} \\ y_n &= \frac{W_{n0}}{W_n} \end{aligned}\right\} \tag{4-33}$$

The parameters W_{n0}, $n = 1, 2$, are the bandwidths of the carrier-tracking loops at the "design point" [Eq. (3-13)], and W_n, $n = 1, 2$, is the bandwidth of the IF filter that precedes the carrier-tracking loops. Further, the parameters r_{n0} and μ_n are given by

$$r_{n0} = \frac{\alpha_{n0} K_n \tau^2_{2n}}{\tau_{1n}}, \qquad \mu_n = \frac{\alpha_{n0}}{\alpha_{nn}} \tag{4-34}$$

where α_{nn} are the limiter suppression factors given in Eqs. (3-4) and (3-5) with a slight change in notation to accommodate the two-way system model. Finally, G is the static phase gain of the vehicle receiver, and $K_R(k_1, k_2, \beta)$ is given by

$$K_R(k_1, k_2, \beta) = \frac{k_2}{k_1}\left[\frac{2k_1\beta + 4\beta^2(1+\beta) + \beta^3(1+\beta)k_1k_2 + 2k_2\beta^4}{k_1^2 + 2k_1\beta + 2\beta(k_1 + k_2 - k_1k_2) + 2\beta^3k_2 + k_2^2\beta^4}\right]\left(\frac{1}{r_{10} + 1}\right) \tag{4-35}$$

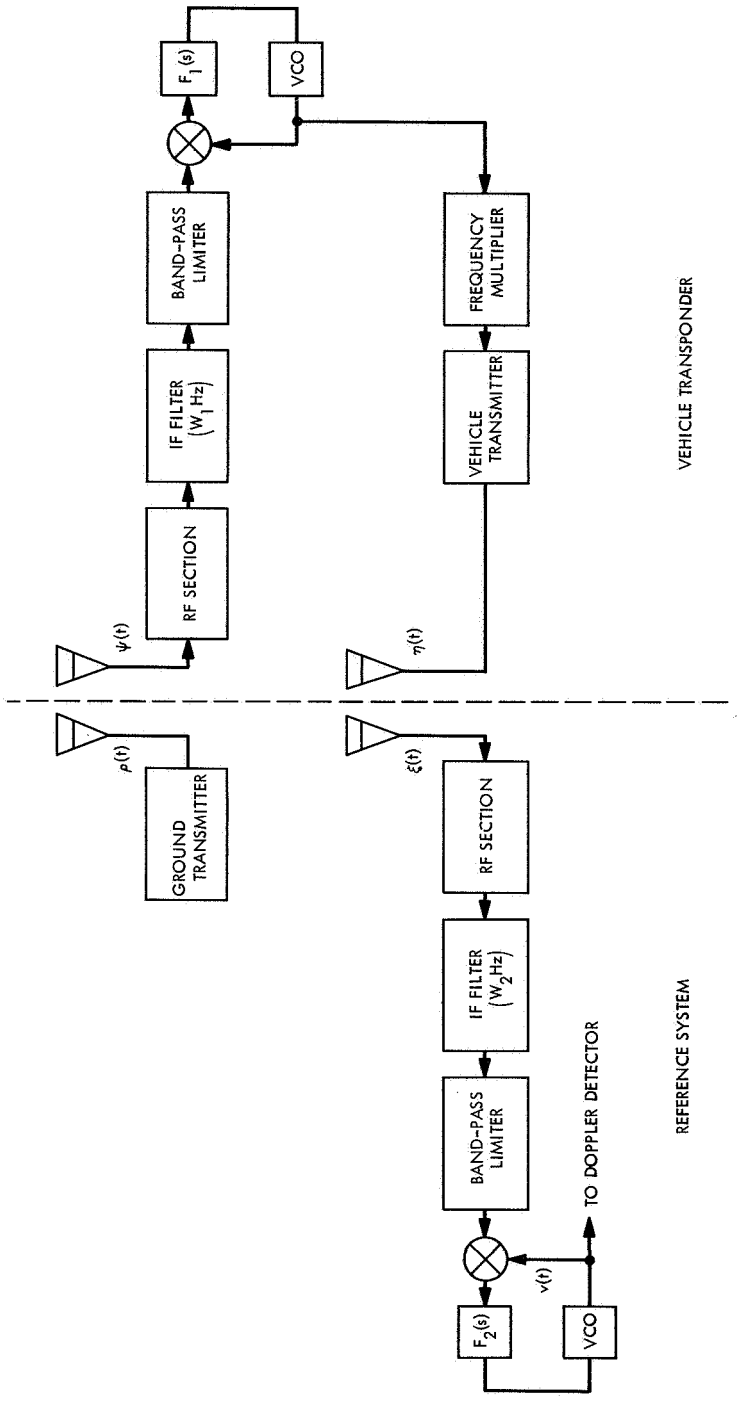

Fig. 4-7. Two-way-doppler and phase-measuring system with carrier-tracking loops preceded by BPLs

where

$$k_n = 2\mu_n / r_{n0}$$

and

$$\beta = \frac{W_{10}(r_{20}+1)}{W_{20}(r_{10}+1)}$$

Plotted in Fig. 4-8 is Eq. (4-35) vs β for various values of the signal-to-noise ratio in the "design-point" loop bandwidths of the vehicle's and ground receiver's carrier-tracking loops; limiters are present in both receivers. Equation (4-31) is plotted in Fig. 4-9 against various values of the signal-to-noise ratio in the "design-point" loop bandwidths of the vehicle's and ground receiver's carrier-tracking loops. It may be shown that this plot is independent of y for the cases of greatest interest in practice. Linear PLL theory is assumed, and BPLs are present in the system. The performance of one-way phase-measuring links may be obtained from the above equations by allowing $\alpha_{1\ell}$ to approach infinity.

V. Two-Way-Tracking Phase Error Where the Carrier-Tracking Loops Are Preceded by BPLs (Nonlinear PLL Theory)

The distribution of the phase error ϕ_2 may be modeled in a manner analogous to that employed in Section III of this chapter. Thus, when BPLs precede the carrier-tracking loops, the distribution of the phase error is well approximated by

$$p(\phi_2) = \frac{I_0(|\alpha_{1\ell} + \alpha_{2\ell}\exp(j\phi_2)|)}{2\pi I_0(\alpha_{1\ell}) I_0(\alpha_{2\ell})}, \qquad |\phi| \le \pi \tag{4-36}$$

where $\alpha_{1\ell}$ and $\alpha_{2\ell}$ are defined in Eq. (4-32). The variance of Eq. (4-36) is of interest in practice, i.e.,

$$\sigma_2^2 = \int_0^{\pi} \phi^2 \frac{I_0[(\alpha_{1\ell}^2 + \alpha_{2\ell}^2 + 2\alpha_{1\ell}\alpha_{2\ell}\cos\phi_2)^{1/2}]}{\pi I_0(\alpha_{1\ell}) I_0(\alpha_{2\ell})}\, d\phi_2 \tag{4-37}$$

and becomes, upon carrying out the integration,

$$\sigma_{r2}^2 = \sigma_{\phi 2}^2 = \frac{\pi^2}{3} + 4\sum_{k=1}^{\infty} \frac{(-1)^k I_k(\alpha_{1\ell}) I_k(\alpha_{2\ell})}{k^2 I_0(\alpha_{1\ell}) I_0(\alpha_{2\ell})} \tag{4-38}$$

Plotted in Fig. 4-10 is Eq. (4-38) for various system mechanizations. The variance shown in this figure exists in the "design-point" loop bandwidths of the vehicle's and ground receiver's carrier-tracking loops. It may be shown that this plot is independent of y for the cases of greatest interest in practice. Nonlinear PLL theory is assumed, and BPLs are present in the system.

VI. Comparison of the Performance of One-Way and Two-Way Phase-Measuring Systems Where BPLs Are Present (Linear PLL Theory)

Frequently in the design of two-way phase-measuring systems, comparison of the performance of a one-way system with a two-way system is desirable. For the purposes here, this comparison is predicated on the ratio of the variance of the two-way phase error to the variance of the one-way phase error. In the linear PLL theory that uses carrier-tracking loops preceded by BPLs,

$$\frac{\sigma_{r2}^2}{\sigma_{r1}^2} = \frac{\sigma_{\phi 2}^2}{\sigma_{\phi 1}^2} = R_{21} = 1 + \frac{\alpha_{2\ell}}{\alpha_{1\ell}} \tag{4-39}$$

In Fig. 4-11 the function R_{21} is plotted against the signal-to-noise ratio in the ground receiver's "design-point" loop bandwidth for various system mechanizations. Results are given in this figure for various values of the signal-to-noise ratio x_1 in the "design-point" loop bandwidth of the vehicle's carrier-tracking loop. Linear PLL theory is assumed in Fig. 4-11, and BPLs are present in the system. Note that this comparison assumes that the frequency and phase of the downlink carrier in the one-way phase-measuring system is precisely known. In practice, this assumption is not valid; consequently, information relative to the frequency and phase of the spacecraft oscillators must be telemetered back to the reference system with extreme accuracy.

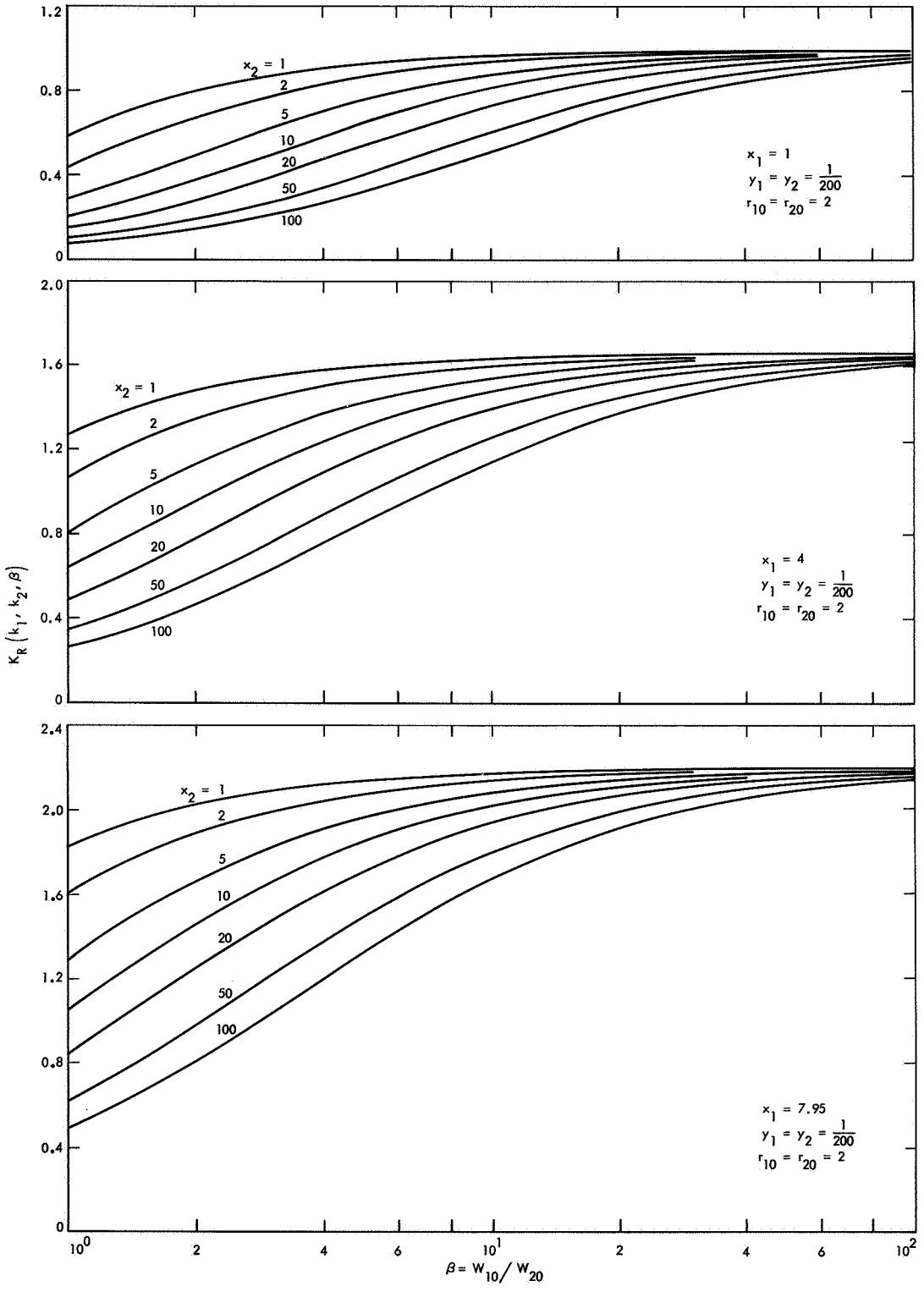

Fig. 4-8. The function $K_R(k_1, k_2, \beta)$ vs β for various values of the signal-to-noise ratio

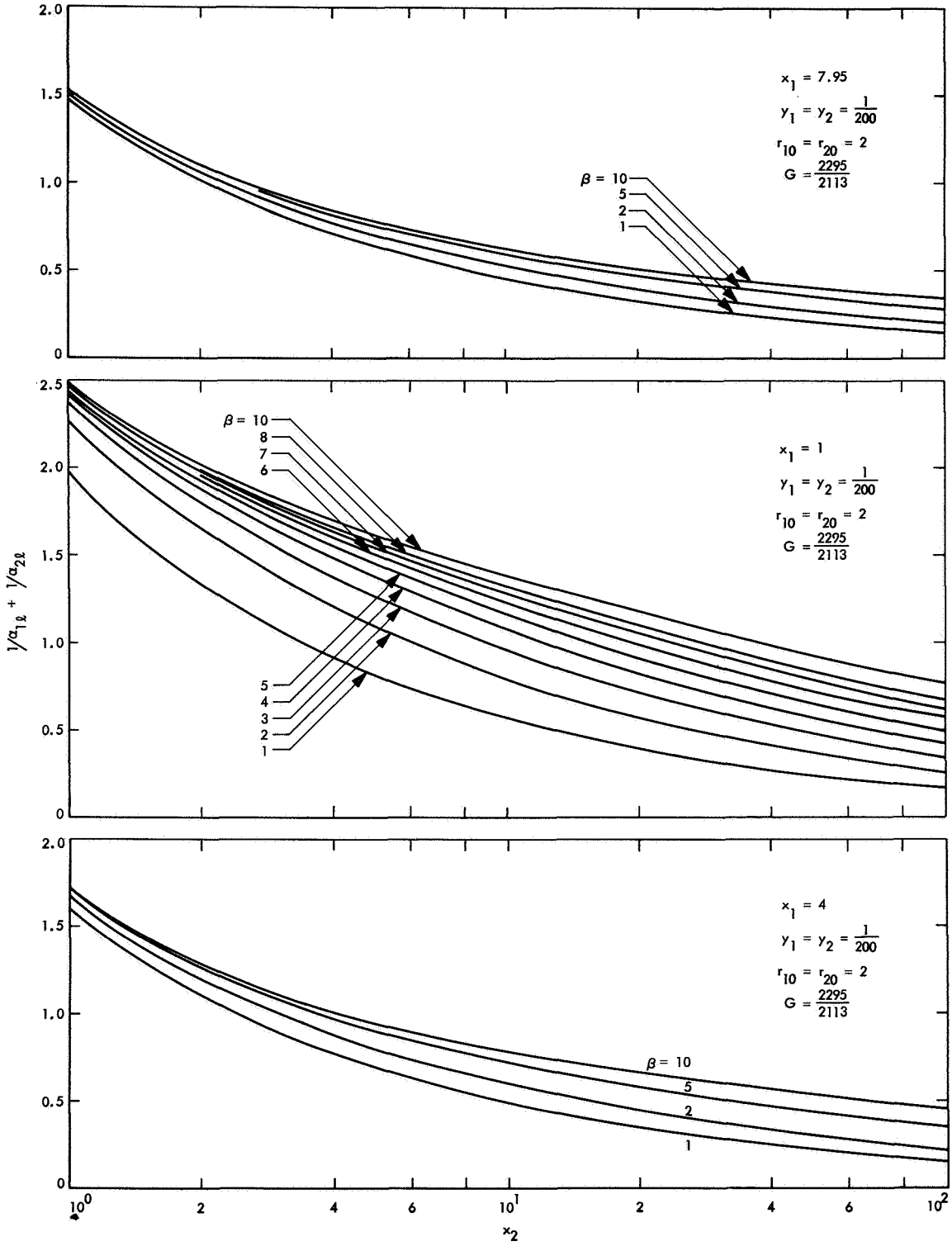

Fig. 4-9. Variance of the two-way phase error σ^2_{r2} vs the signal-to-noise ratio; linear PLL theory is assumed with BPLs preceding the loop

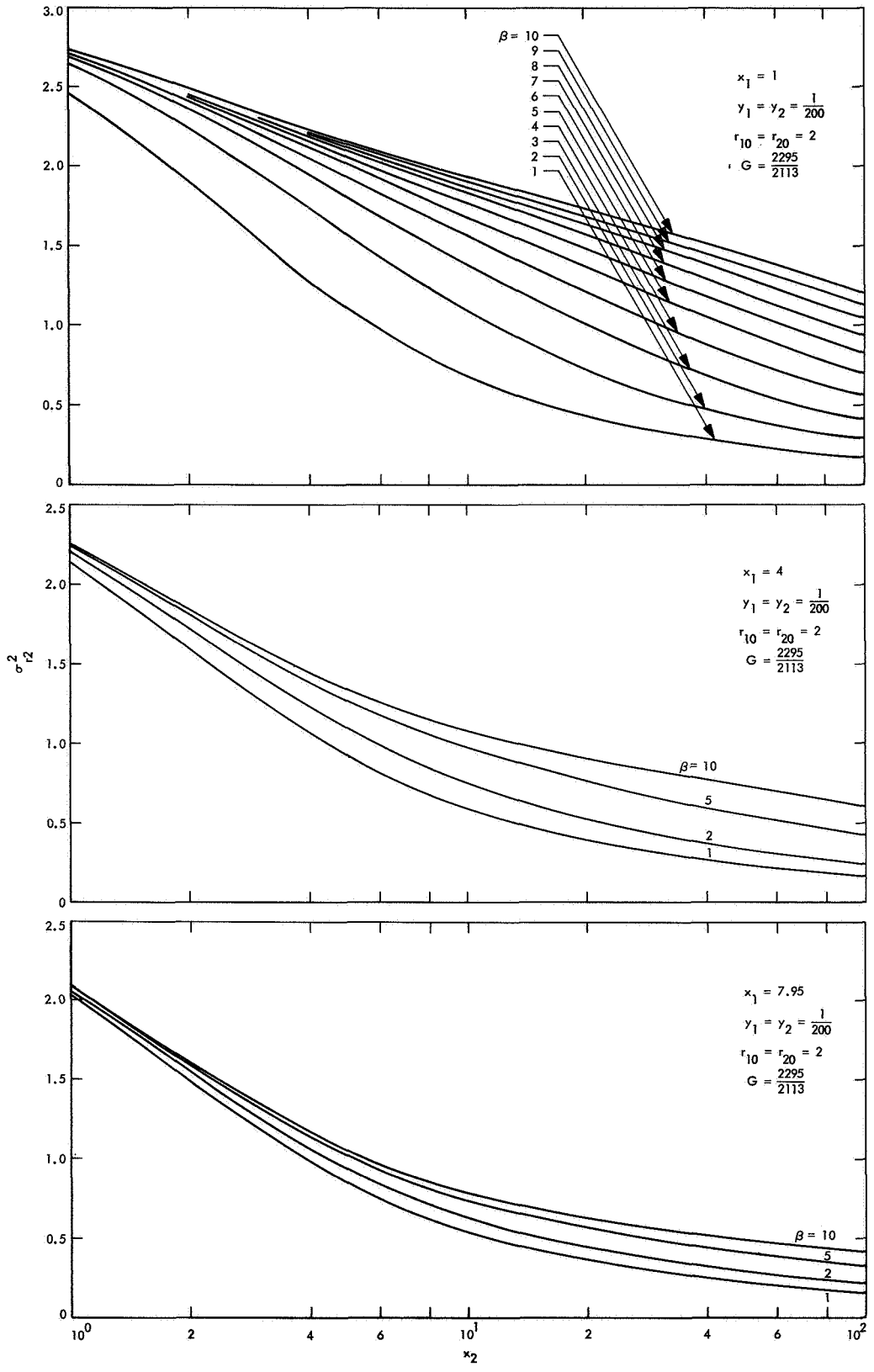

Fig. 4-10. Variance of the two-way phase error $\sigma^2_{\phi_2}$ vs the signal-to-noise ratio; nonlinear PLL theory is assumed with BPLs preceding the loop

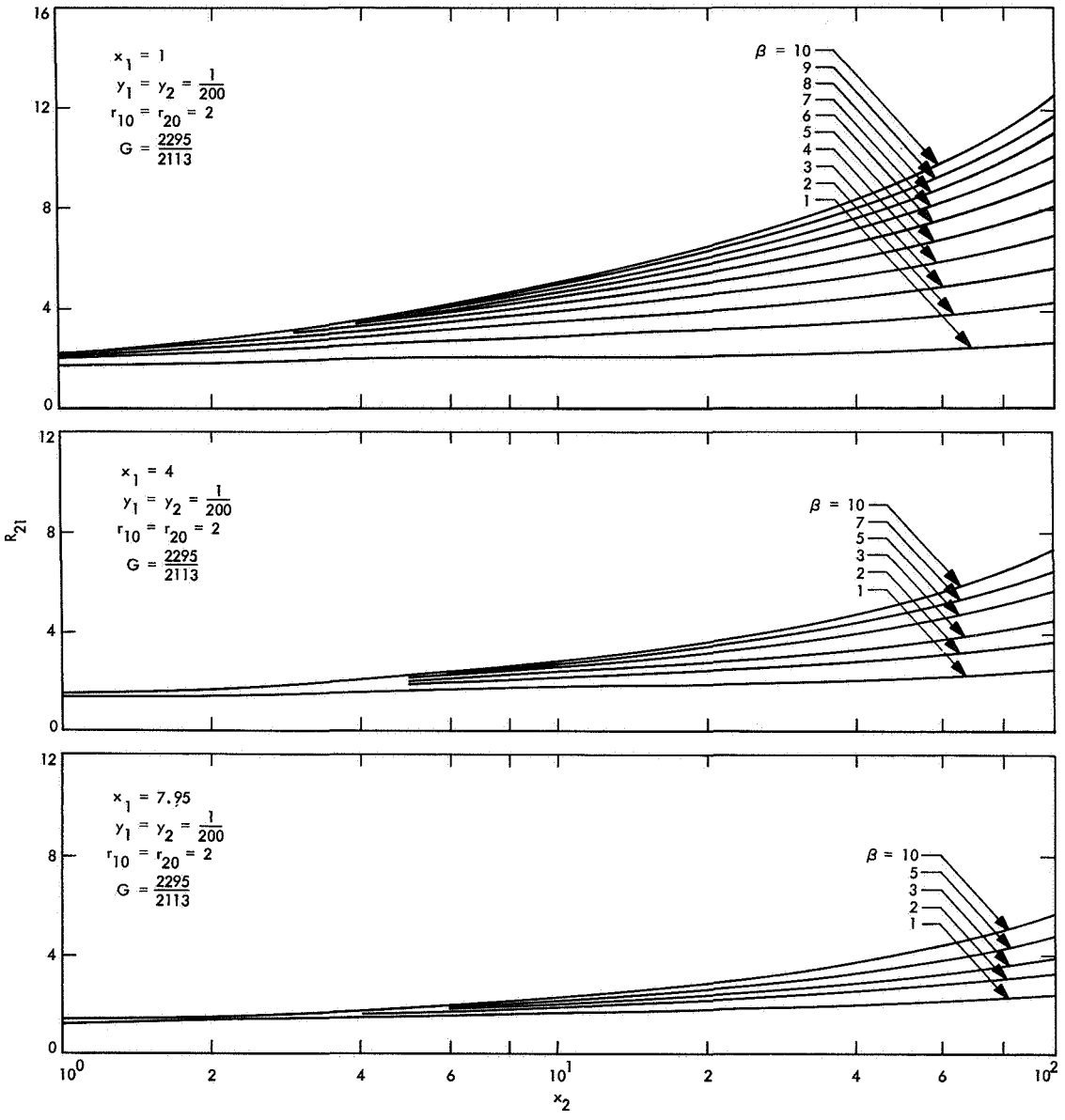

Fig. 4-11. Comparison of one-way and two-way phase-measuring systems vs the signal-to-noise ratio

Reference

4-1. Lindsey, W. C., "Optimal Design of One-Way and Two-Way Phase-Coherent Communication Systems," *IEEE Transactions on Communication Technology*, Vol. COM-14, pp. 418–431, Aug. 1966.

Chapter 5
Doppler Measurements in One-Way and Two-Way Phase-Coherent Communication Systems

In deep-space communication systems, a major function that must be performed with extreme accuracy is tracking. Tracking information consists of the vehicle's velocity, range, and angular position. Velocity of the vehicle is usually based on an estimate of the received signal's doppler shift in frequency. This doppler shift, which is proportional to the velocity of the vehicle along a line connecting the vehicle to the reference system, is sometimes referred to as the doppler velocity, range rate, or slant velocity; in this discussion, the parameter will be referred to as doppler. Doppler may be used to accurately specify the flight path or trajectory of the vehicle, and it is of fundamental importance in all uses of telemetry data.

There are several techniques for measuring doppler; the one considered in this section is the measurement of a two-way doppler shift by transmitting a known signal to the vehicle and coherently transponding the observed signal back to the reference system. One-way-doppler measurement is made by transmitting a signal from a free-running oscillator on board the vehicle and estimating the received doppler shift. One-way doppler is, of course, inferior to two-way doppler because the frequency of the reference oscillator on board the vehicle must be known *a priori* at the reference system. In practice, owing to drifts in the frequency source because of variations in the physical environment, the frequency radiated from the vehicle is not precisely known. Thus, to obtain accurate doppler measurements in a one-way-doppler system, separate telemetered information about the spacecraft or vehicle oscillators is required. Consequently, from a practical point of view, two-way doppler is more attractive than one-way doppler.

A two-way-doppler measuring system determines the vehicle's velocity from the two-way-doppler shift of the uplink carrier frequency. To measure this doppler shift, coherence of the uplink carrier frequency through the vehicle transponder and back to the ground or reference receiver is necessary. This uplink carrier frequency is compared in frequency with a continuing sample of the uplink frequency in the velocity extraction unit. The velocity extraction unit measures doppler by counting, for a preset period, the number of cycles in the sum of the doppler shift and a known frequency offset or bias.

This section will develop a theory upon which the performance of a two-way-doppler measuring system may be designed and evaluated. The theory presented includes the effects of BPLs in both the vehicle and the reference systems, and the effects of nonlinear behavior of the PLLs on system design. The linear PLL theory with and without BPLs preceding the PLLs is also considered.

I. Basic System Model

Figure 4-1 describes the simplest mechanization of a two-way-doppler measuring system. The reference system emits, on the uplink, the waveform

$$\rho(t) = \sqrt{2P_{c2}} \sin \omega_0 t \tag{5-1}$$

After transmission, the channel introduces an arbitrary and unknown phase shift θ_1 in the transmitted waveform and further disturbs $\rho(t)$ with additive white Gaussian noise $n_1(t)$ of the single-sided spectral density N_{10} W/Hz. There occurs in the vehicle, then, the doppler-shifted, phase-shifted, noise-corrupted waveform

$$\psi(t) = \sqrt{2P_{c1}} \sin (\omega_1 t + \theta_1) + n_1(t) \tag{5-2}$$

The additive noise process $n_1(t)$ may be represented by

$$n_1(t) = x_1(t) \cos (\omega_1 t + \theta_1) + y_1(t) \sin (\omega_1 t + \theta_1) \tag{5-3}$$

where $x_1(t)$ and $y_1(t)$ are statistically independent, stationary white Gaussian noise processes of single-sided spectral density N_{10} W/Hz. The vehicle coherently tracks, by means of a narrowband PLL, the carrier component, and produces the estimate

$$z(t) = \sqrt{2} \cos (\omega_1 t + \hat{\theta}_1) \tag{5-4}$$

where $\hat{\theta}_1$ is the PLL estimate of θ_1.

The carrier for the downlink in a two-way-doppler measuring system is derived from the vehicle's carrier-tracking loop. Thus, on the downlink, we transmit

$$\eta(t) = \sqrt{2P_{c2}} \sin (\omega_{10} t + \hat{\theta}_1) \tag{5-5}$$

and observe, at the reference system, the doppler-shifted, phase-shifted, noise-corrupted waveform

$$\xi(t) = \sqrt{2P_{c2}} \sin (\omega_2 t + \hat{\theta}_1 + \theta_2) + n_2(t) \tag{5-6}$$

where $n_2(t)$ is stationary white Gaussian noise of the single-sided spectral density N_{20} W/Hz, and $\omega_{10} = G\omega_1$. Here G denotes the static phase gain of the vehicle transponder. A convenient representation for $n_2(t)$ is given by

$$n_2(t) = x_2(t) \cos (\omega_2 t + \hat{\theta}_1 + \theta_2) + y_2(t) \sin (\omega_2 t + \hat{\theta}_1 + \theta_2) \tag{5-7}$$

where $x_2(t)$ and $y_2(t)$ are statistically independent and white Gaussian noise processes. The reference receiver tracks the carrier component in $\xi(t)$, which provides the receiver with the estimate

$$v(t) = \sqrt{2} \cos (\omega_2 t + \hat{\theta}_2) \tag{5-8}$$

The quantity $\hat{\theta}_2$ is the PLL estimate of $\hat{\theta}_1 + \theta_2$.

In the design of such a system, the mean-squared value of the two-way-doppler error ϕ_{d2} is a significant parameter:

$$\sigma^2_{\phi_{d2}} = \overline{(\hat{\theta}_2 - \theta_0)^2} = \overline{\phi^2_{d2}} \tag{5-9}$$

where the bar denotes the mathematical expectation, and θ_0 is the phase of the transmitted carrier (assumed to be zero). In Section II of this chapter, the doppler error ϕ_{d2} and its relationship to the various system parameters are considered. The investigation begins by using the linear PLL theory; in a later part of this chapter, the problem is remodeled to permit study of nonlinear PLL effects. Finally, the doppler error where BPLs precede the vehicle's reference system carrier-tracking loop is considered.

II. Two-Way-Doppler Error (Linear PLL Theory)

In linearized form, the important features of the system of Fig. 4-1 are depicted in Fig. 4-2. (In Figs. 4-1 and 4-2, s denotes the Laplace transform variable.) The parameter G is the static phase gain of the vehicle transponder; this gain is determined by the ratio of the output carrier frequency to the input carrier frequency. The filter functions $H_n(s)$, where $n = 1, 2$, are the closed-loop transfer functions of the system's carrier-tracking loops. The form of the filters is described in detail in Eqs. (2-13) and (4-14).

The two-way-doppler phase error ϕ_{d2} is defined by the difference between the reference-receiver output phase θ_2 and the original phase of the transmitter carrier $\theta_0 = 0$. Thus, the spectral density of the doppler error due to noise alone at the reference receiver output is (in the Laplace transform notation)

$$\phi_{d2}(s)\phi_{d2}(-s) = \frac{N_{10}G^2}{2P_{c1}} | H_1(s)H_2(s) |^2 + \frac{N_{20}}{2P_{c2}} | H_2(s) |^2 \tag{5-10}$$

and the mean-squared value of the doppler error is

$$\sigma^2_{\phi_{d2}} = \frac{1}{2\pi j}\left[\frac{N_{10}G^2}{2P_{c1}}\int_{-j\infty}^{j\infty} |\, H_1(s)H_2(s)\,|^2\, ds + \frac{N_{20}}{2P_{c2}}\int_{-j\infty}^{j\infty} |\, H_2(s)\,|^2\, ds\right] \tag{5-11}$$

Substituting Eq. (4-14) into Eq. (5-11) and carrying out the integration (Ref. 5-1), we have

$$\sigma^2_{\phi_{d2}} = \frac{1}{d_1} + \frac{1}{d_2} \tag{5-12}$$

where

$$d_1 = \frac{2P_{c1}}{N_{10}W_{L1}} \times \frac{1}{G^2K_D(r_1, r_2, \beta)}$$

$$d_2 = \frac{2P_{c1}}{N_{20}W_{L2}}$$

and

$$K_D(r_1,r_2,\beta) = \frac{1}{r_1+1}\left[\frac{r_2(r_1+1) + r_1(r_1+r_2+r_1r_2)(\beta+\beta^2) + r_1(r_1r_2+r_1)\dfrac{\beta^2}{r_2}}{r_2 + r_1r_2\beta + r_1(r_1+r_2-2)\beta^2 + r_1^2\beta^3 + r_1^2\dfrac{\beta^4}{r_2}}\right] \tag{5-13}$$

$$\beta = \frac{W_{L1}(r_2+1)}{W_{L2}(r_1+1)}$$

The function $K_D(r_1, r_2, \beta)$ has been computed for a system without BPLs, and the results are plotted in Fig. 5-1 for the various values of system damping $r_1 = r_2 = r$ and β. It is evident from Fig. 5-1 that the parameters r_1, r_2, and β are important ones to consider in the design of two-way-doppler measuring systems.

Before the nonlinear behavior of the doppler-measuring system is characterized, the performance of a system that makes a two-way-doppler measurement should be compared with the performance of a system that makes a one-way-doppler measurement. The ratio of the mean-squared value of the two-way-doppler phase error to the mean-squared value of the one-way-doppler phase error is given by

$$Q_{21} = \frac{\sigma^2_{\phi_{d2}}}{\sigma^2_{\phi_{d1}}} = \frac{\dfrac{1}{d_1} + \dfrac{1}{d_2}}{\dfrac{1}{d_2}} = 1 + \frac{d_2}{d_1} \tag{5-14}$$

which becomes

$$Q_{21} = 1 + \frac{N_{10}W_{L1}}{2P_{c1}} \times G^2K_D(r_1, r_2, \beta) \tag{5-15}$$

This comparison is made in Fig. 5-2 for various system mechanizations; the linear PLL theory is assumed in the figure, and no BPLs are present in the system.

III. Two-Way-Doppler Error (Nonlinear PLL Theory)

The exact nonlinear PLL theory that pertains to the two-way-doppler measurement appears formidable; however, an approximate model for the probability distribution of the two-way-doppler error $\phi_{d2} = \phi_d$ may be developed on the basis of the nonlinear theory of PLLs and the measurements presented in Chapter 2. The accuracy with which the model predicts the performance of the doppler-measuring system of Fig. 4-1 is determined

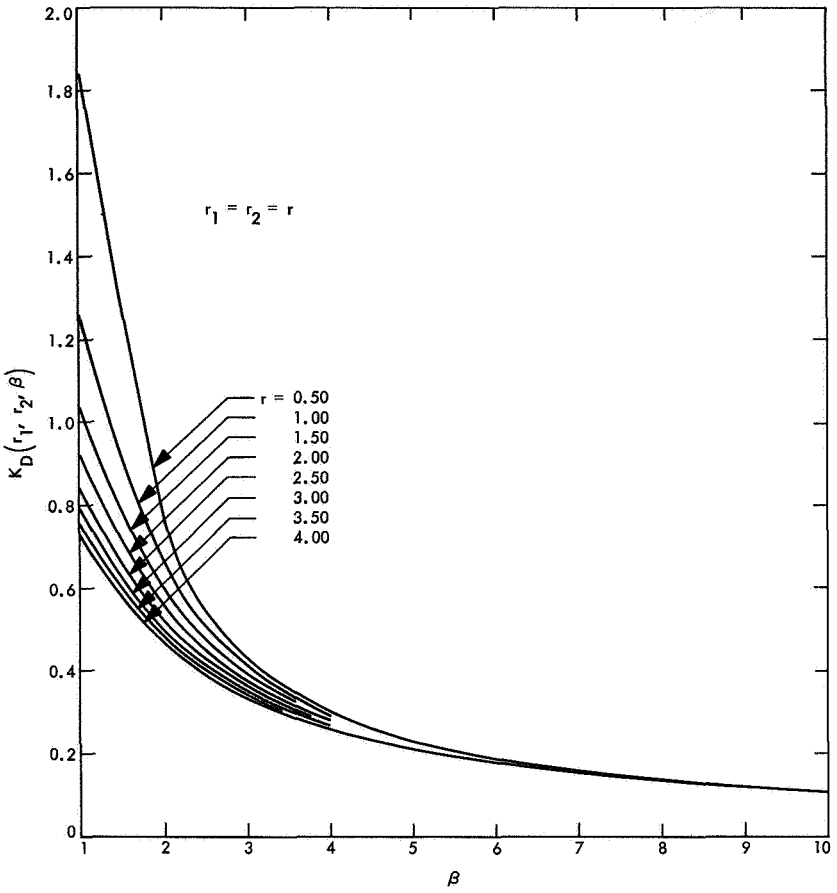

Fig. 5-1. The function $K_D(r_1, r_2, \beta)$ vs $\beta = W_{L1}/W_{L2}$

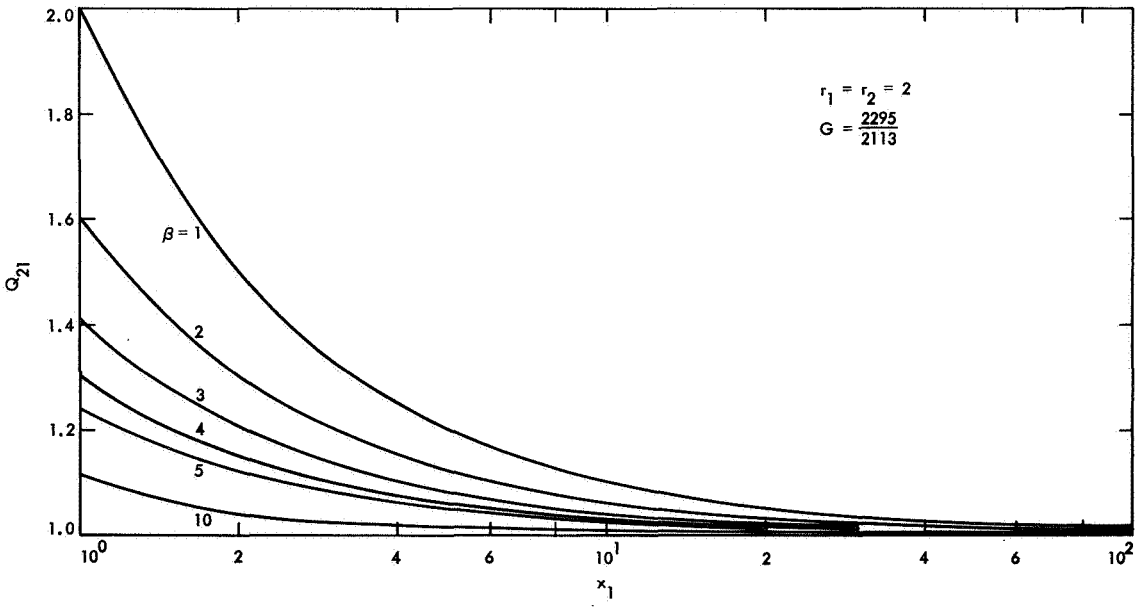

Fig. 5-2. Comparison of the performance of one-way- and two-way-doppler measuring systems for various values of $\beta = W_{L1}/W_{L2}$

by results obtained in the laboratory. Unfortunately, these results are not available at present; however, the distribution (to be given below) of the doppler-error checks at the extremes of high and low signal-to-noise ratios has been verified, which leaves suspect only the region between.

On the basis of the results in Chapter 2, the distribution of the two-way-doppler error can be approximated by (Ref. 5-2)

$$p(\phi_d) = \frac{I_0[\,|\,d_1 + d_2 \exp(j\phi_2)\,|\,]}{2\pi I_0(d_1) I_0(d_2)}, \qquad |\,\phi\,| \leq \pi \tag{5-16}$$

where $I_0(x)$ is the imaginary Bessel function of zero order and of argument x, and d_1 and d_2 are defined in Eq. (5-12). This model distribution is valid only if G is approximately equal to unity, which is the case of greatest practical interest. The validity of this distribution as a model for the two-way-doppler error may be checked using the limiting cases of high and low signal-to-noise ratios. For large signal-to-noise ratios in the uplink and downlink carrier-tracking loops, the distribution Eq. (5-16) becomes Gaussian with zero mean and a variance of $d_1^{-1} + d_2^{-1}$. Thus, for large signal-to-noise ratios, the distribution checks with the linear PLL theory in Section 4-II.

For weak signal conditions on either the uplink or the downlink, or both, Eq. (5-16) becomes uniformly distributed:

$$\lim_{d_1 \text{ or } d_2 \to 0} p(\phi_d) = \frac{1}{2\pi}, \qquad |\,\phi_{d2}\,| < \pi \tag{5-17}$$

This agrees with what might be expected for weak signal conditions, and therefore the model for doppler-error distribution checks at the end points. Between these points, the validity of using $p(\phi_d)$ as the distribution of doppler error must be checked through laboratory measurement.

The variance of this distribution is important in practice:

$$\sigma_{\phi_d}^2 = \int_{-\pi}^{\pi} \phi_d^2\, p(\phi_d)\, d\phi_d \tag{5-18}$$

Substitution of Eq. (5-16) into Eq. (5-18) leads to the result

$$\sigma_{d2}^2 = \sigma_{\phi_d}^2 = \frac{\pi^2}{3} + 4 \sum_{k=1}^{\infty} \frac{(-1)^k I_k(d_1) I_k(d_2)}{k^2 I_0(d_1) I_0(d_2)} \tag{5-19}$$

Equation (5-19) is plotted in Fig. 4-6 for various values of $d_1 = d_2$. For comparison purposes, results from the linear and nonlinear theory of one-way links are illustrated in Fig. 4-6 (i.e., $n = 1$).

IV. Two-Way-Doppler Error Where the Carrier-Tracking Loops Are Preceded by BPLs (Linear PLL Theory)

In practice, and for the reasons given in Section 3-I, BPLs always precede the carrier-tracking loops. Figure 4-7 illustrates a typical mechanization of a practical two-way-doppler measuring system.

Employing the linear PLL theory given in Chapter 3 and Eq. (5-11), we see that the variance of the two-way-doppler error is

$$\sigma_{\phi_d}^2 = \frac{1}{d_{1\ell}} + \frac{1}{d_{2\ell}} \tag{5-20}$$

where

$$\left.\begin{aligned} d_{1\ell} &= \frac{2P_{c1}}{W_{10}N_{10}} \times \frac{1}{G^2 \Gamma_1 K_D(k_1, k_2, \beta)} \\ d_{2\ell} &= \frac{2P_{c2}}{N_{20}W_{20}} \left(\frac{1 + r_{20}}{1 + r_{20}/\mu_2}\right) \frac{1}{\Gamma_2} \end{aligned}\right\} \tag{5-21}$$

and Γ_n, $n = 1, 2$, are the limiter performance factors given by Eq. (4-33). The parameters W_{n0}, $n = 1, 2$, are the bandwidths of the carrier-tracking loops at the "design point" [Eq. (3-13)], and W_n, $n = 1, 2$, is the bandwidth of the IF filter that precedes the PLL. Further, the parameters r_{n0} and μ_n, $n = 1, 2$, are defined in Eq. (4-34). The function $K_D(k_1, k_2, \beta)$ is given by

$$K_D(k_1, k_2, \beta) = \frac{1}{r_{10} + 1} \left[\frac{k_1(2 + k_1) + 2(k_1 + k_2 + 2)(\beta + \beta^2) + k_2(2 + k_2)\beta^3}{k_1^2 + 2k_1\beta + 2(k_1 + k_2 - k_1k_2)\beta^2 + 2k_2\beta^3 + k_2^2\beta^4}\right] \tag{5-22}$$

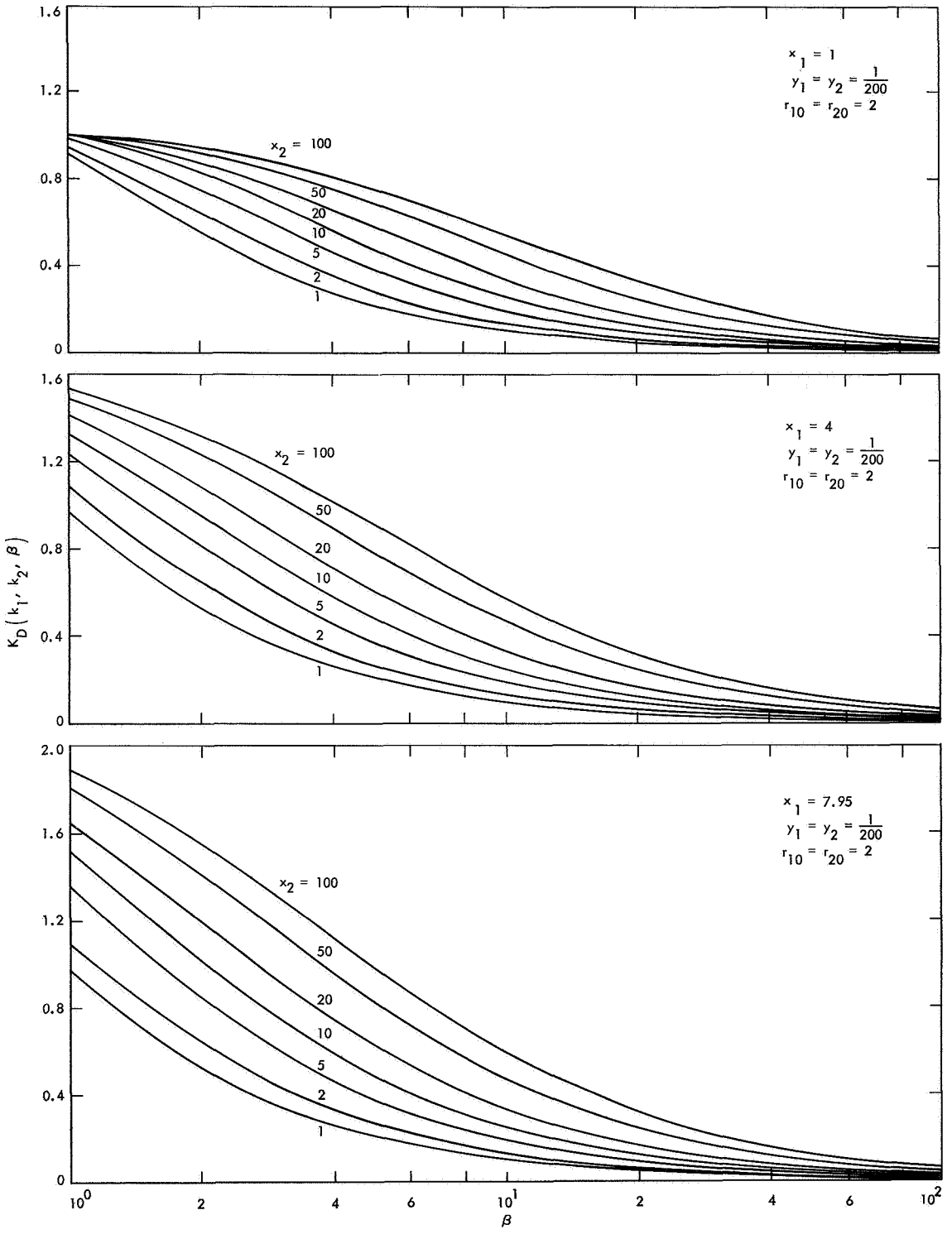

Fig. 5-3. The function $K_D(k_1, k_2, \beta)$ vs $\beta = W_{10}/W_{20}$

where

$$k_n = \frac{2\mu_n}{r_{n0}}$$

and

$$\beta = \frac{W_{10}(r_{20}+1)}{W_{20}(r_{10}+1)}$$

Plotted in Fig. 5-3 is Eq. (5-22) vs β for various values of the signal-to-noise ratios in the "design-point" loop bandwidth of the vehicle's and ground receiver's carrier-tracking loops. The performance of a one-way-doppler measuring system may be obtained from Eqs. (5-20) and (5-21) by letting $d_{1\ell}$ approach infinity.

Plotted in Fig. 5-4 is Eq. (5-20) for various system mechanizations; for other values of y of interest in practice, the results are, for practical purposes, the same.

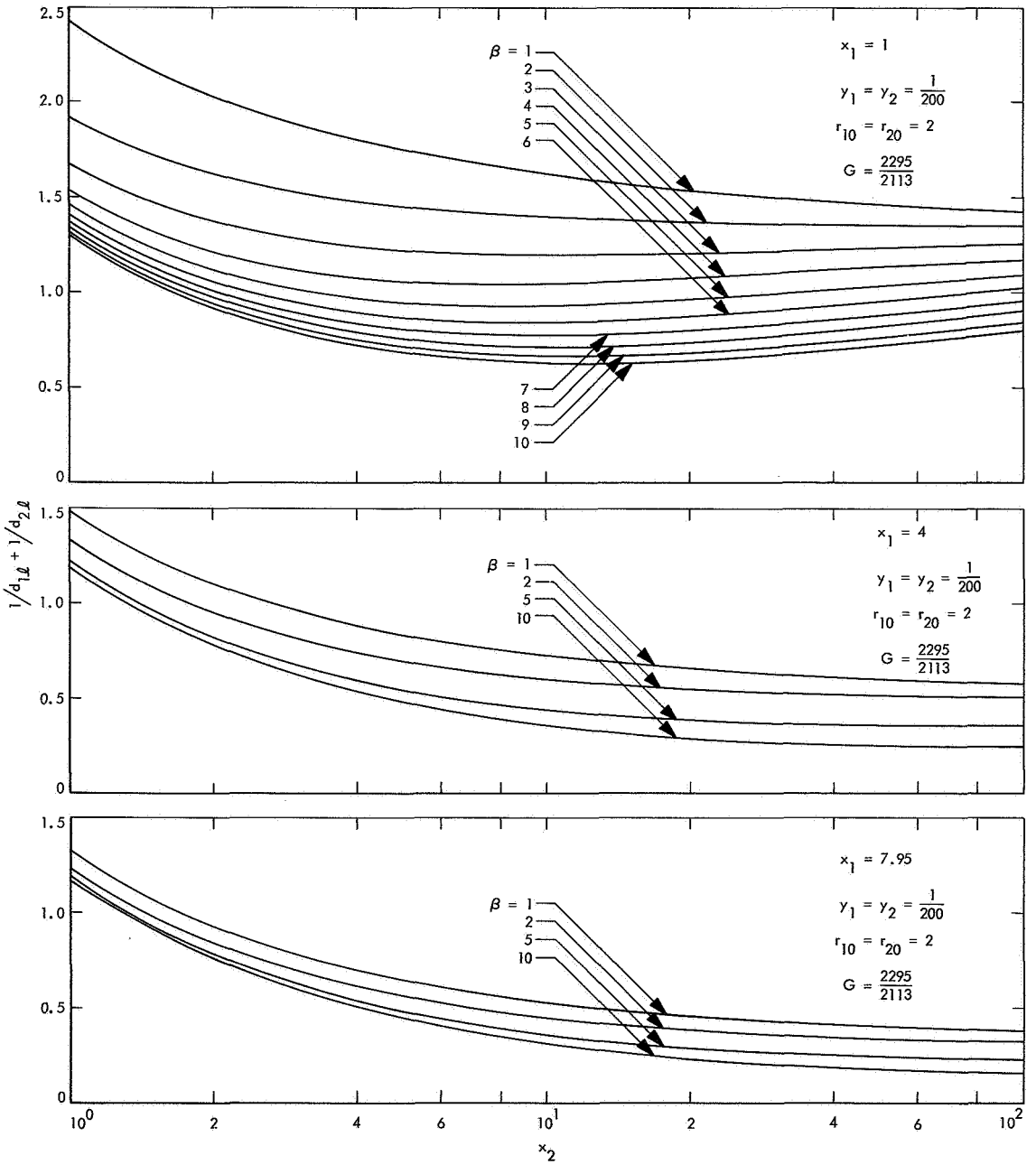

Fig. 5-4. Variance of the two-way-doppler error σ_{d2}^2 vs the signal-to-noise ratios existing in the "design-point" loop bandwidth of the vehicle and ground receiver's carrier-tracking loops (linear PLL theory)

Linear PLL theory is assumed in the figure, and BPLs are present in the system. The resultant behavior may be attributed to the increase in the ground receiver's loop bandwidth as the signal-to-noise ratio on the downlink increases.

V. Two-Way-Doppler Error Where the Carrier-Tracking Loops Are Preceded by BPLs (Nonlinear PLL Theory)

The distribution of the doppler error ϕ_d may be modeled in a manner analogous to that employed in Section 4-III. Thus, when bandpass limiters precede the carrier-tracking loops, distribution of the phase error is well approximated by (Refs. 5-1 and 5-2)

$$p(\phi_d) = \frac{\mathrm{I}_0[\,|\, d_{1\ell} + d_{2\ell} \exp(j\phi_d)\,|\,]}{2\pi \mathrm{I}_0(d_{1\ell})\mathrm{I}_0(d_{2\ell})}, \qquad |\,\phi_d\,| \leq \pi \tag{5-23}$$

where $d_{1\ell}$ and $d_{2\ell}$ are defined in Eq. (5-21). The variance of Eq. (5-23) is

$$\sigma^2_{\phi_d} = \int_0^{\pi} 2\phi_d^2\, p(\phi_d)\, d\phi_d \tag{5-24}$$

Substitution of Eq. (5-23) in Eq. (5-24) leads to the expression

$$\sigma^2_{\phi_d} = \frac{\pi^2}{3} + 4\sum_{k=1}^{\infty} \frac{(-1)^k \mathrm{I}_k(d_{1\ell})\mathrm{I}_k(d_{2\ell})}{k^2 \mathrm{I}_0(d_{1\ell})\mathrm{I}_0(d_{2\ell})} \tag{5-25}$$

Plotted in Fig. 5-5 is Eq. (5-25) for various system mechanizations; the conditions of this figure are those of Fig. 5-4, except that the nonlinear PLL theory is assumed. The behavior of the doppler variance as a function of the signal-to-noise ratio in the "design-point" loop bandwidth x_2 may be attributed again to increase in the bandwidth of the ground receiver's carrier-tracking loop as the downlink signal-to-noise ratio increases.

VI. Comparison of the Performance of One-Way- and Two-Way-Doppler Systems Where BPLs Are Present (Linear PLL Theory)

This comparison is predicated on the basis of the ratio of the variance of the two-way-doppler error to the variance of the one-way-doppler error. Using the linear PLL theory with the carrier-tracking loop preceded by BPLs, we have

$$D_{21} = 1 + \frac{d_{2\ell}}{d_{1\ell}} \tag{5-26}$$

The function D_{21} vs the signal-to-noise ratio in the "design-point" loop bandwidth of the ground receiver for various system mechanizations is illustrated in Fig. 5-6. The results are plotted for various values of the signal-to-noise ratio x that exist in the "design-point" loop bandwidth of the vehicle's carrier-tracking loop. Linear PLL theory is assumed in Fig. 5-6, and BPLs are present in the system. Note that this comparison assumes precise knowledge of the frequency and phase of the downlink carrier in the one-way-doppler measuring system. If the phase and frequency are not known, separate information about the frequency of the spacecraft oscillators must be telemetered back to earth with extreme accuracy to allow the comparison to be made.

References

5-1. Lindsey, W. C., Weber, L. C., "On the Theory of Automatic Phase Control," in *Stochastic Optimization and Control*, pp. 91–133. Edited by H. F. Karreman. John Wiley and Sons, Inc., New York, 1968.

5-2. Lindsey, W. C., "Optimal Design of One-Way and Two-Way Coherent Communications Systems," *IEEE Transactions on Communication Technology*, Vol. COM-14, pp. 418–431, Aug. 1966.

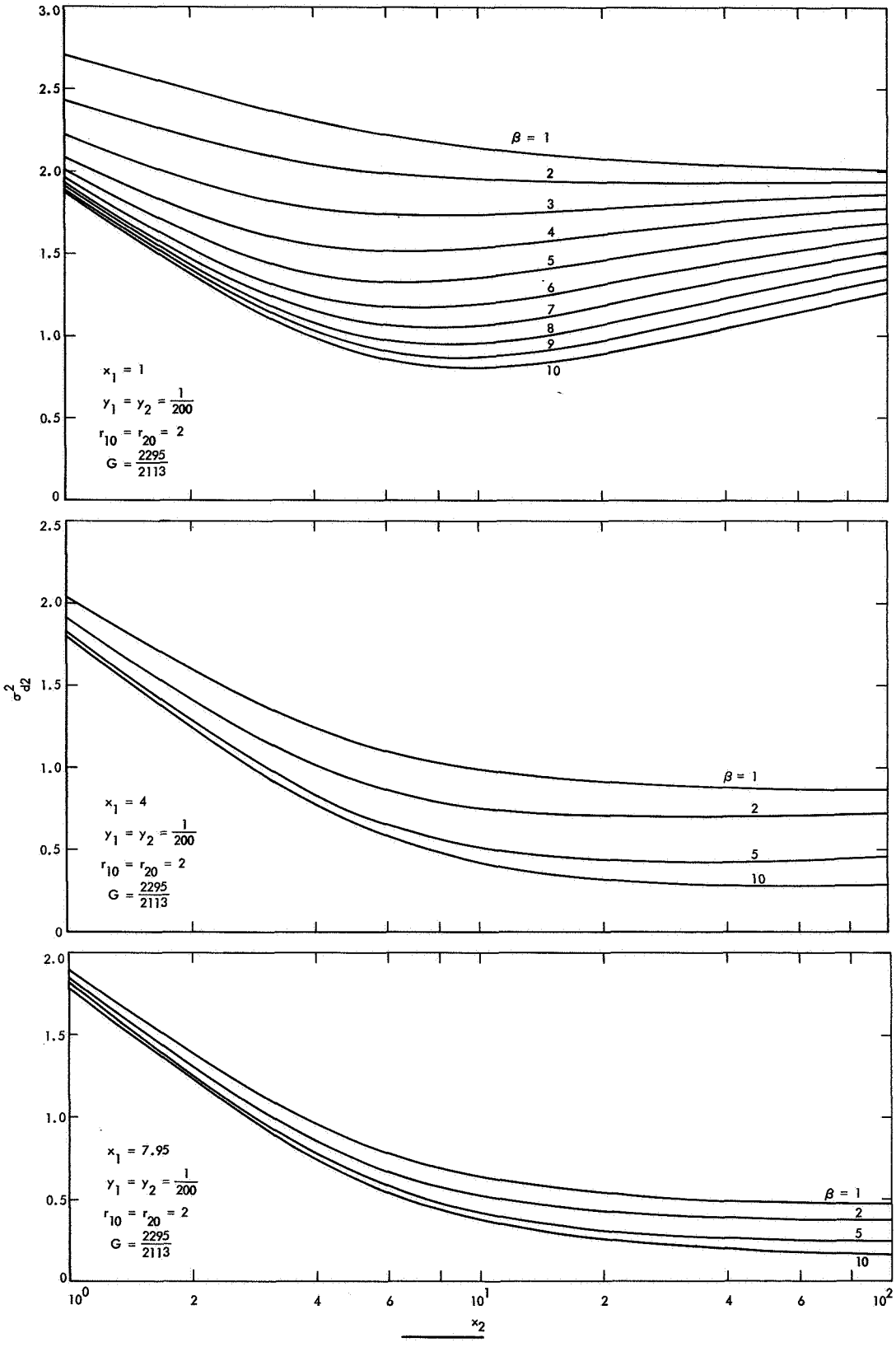

Fig. 5-5. Variance of the two-way-doppler error σ_{d2}^2 vs the signal-to-noise ratios existing in the "design-point" loop bandwidth of the vehicle and ground receiver's carrier-tracking loops (nonlinear PLL theory)

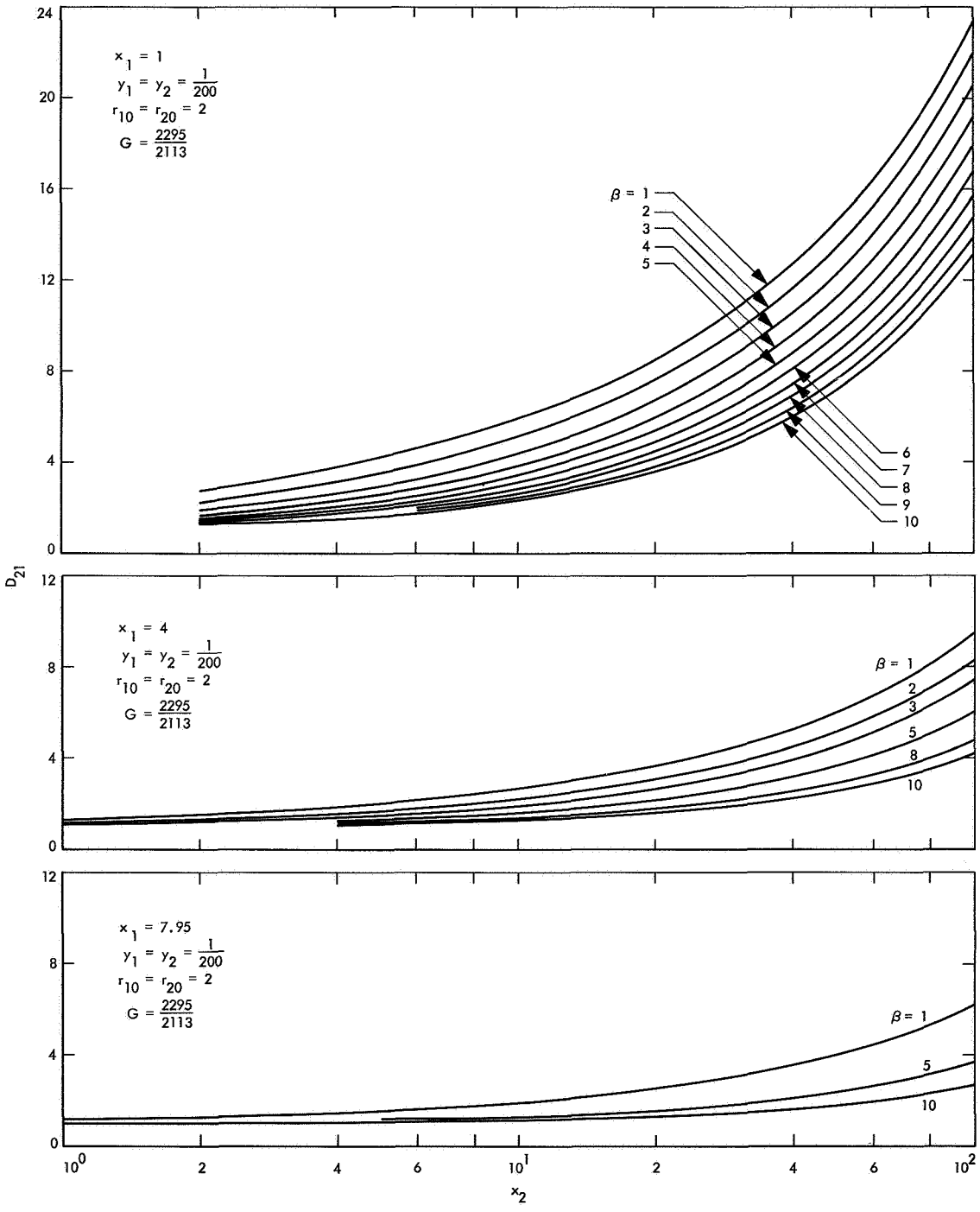

Fig. 5-6. Comparison of one-way- and two-way-doppler measuring systems vs the signal-to-noise ratio

Chapter 6

Downlink Carrier-Suppression Effects Due to Additive Noise on the Uplink in Two-Way Phase-Coherent Carrier-Tracking Systems

The second-moment theory of random processes will be used to determine the effects produced on the downlink carrier by the random modulation that exists on the vehicle's VCO output. This random modulation, $\theta_1(t)$, reduces the power remaining in the downlink carrier component below that value obtained if the system transmitted a clean carrier back to the reference system. In practice, this suppression of the downlink carrier, which may be measured near the end of a mission, is important in the design of a two-way link.

I. Carrier Suppression (Linear PLL Theory)

The waveform transmitted back to the reference system is

$$\eta(t) = \sqrt{2P_{c2}} \sin [\omega_{10}t + \theta_1(t)] \tag{6-1}$$

where $\omega_{10} = G\omega_1$, ω_1 is the received carrier frequency from the uplink, G the static phase gain in the vehicle system, and $\theta_1(t)$ the random phase modulation due to the additive noise on the uplink. The model that follows is valid only if G is approximately equal to unity, which is the case of greatest practical interest. If the linear PLL theory is used, the stationary process $\theta_1(t)$ is well approximated by a normal or Gaussian process with zero mean and a variance $\sigma^2_{\theta_1} = N_{10}W_{L1}G^2/2P_{c1}$. If we denote the covariance function of the phase modulation $\theta_1(t)$ by $K_{\theta_1}(\tau)$ with $K_{\theta_1}(0) = 1$, it may be shown (p. 605 of Ref. 6-1) that the covariance function $K_\eta(\tau)$ of $\eta(t)$ is given by

$$K_\eta(\tau) = P_{c2} \exp \{ - \sigma^2_{\theta_1} [K_{\theta_1}(0) - K_{\theta_1}(\tau)] \} \cos \omega_{10}\tau \tag{6-2}$$

At $\tau = 0$, $K_\eta(0) = P_{c2}$, i.e., as expected, the mean total power is P_{c2} inasmuch as the modulation is entirely in the phase term. The intensity of the downlink carrier component is

$$I_c = K_\eta(\infty) = P_{c2} \exp \left(- \frac{N_{10}W_{L1}G^2}{2P_{c1}} \right) \tag{6-3}$$

and that of the continuum becomes

$$I = K_\eta(0) - K_\eta(\infty) = P_{c2} \left[1 - \exp \left(- \frac{N_{10}W_{L1}G^2}{2P_{c1}} \right) \right] \tag{6-4}$$

For phase modulation, when the process remains Gaussian, it is clear that $I_c > 0$ so that there is always a discrete carrier component, although it may represent a trivial fraction of the total power P_{c2} if σ_{θ_1} is large.

The carrier-suppression factor $\tilde{S}$ is defined as the ratio of the power remaining in the carrier component when the uplink additive noise affects the downlink transmission, to the power remaining in the carrier component when the downlink carrier is derived in the vehicle from a free-running oscillator. Thus, from Eq. (104) we have

$$\tilde{S} = \frac{I_c}{P_{c2}} = \exp\left(-\frac{N_{10}W_{L1}G^2}{2P_{c1}}\right) = \exp\left(-\sigma_{\theta_1}^2\right) \tag{6-5}$$

Plotted in Fig. 6-1 is the carrier-suppression factor vs

$$\sigma_{\theta_1}^{-2} = 2P_{c1}/N_{10}W_{L1}G^2$$

The parameter

$$x_1 = 2P_{c1}/N_{10}W_{L1}$$

is the signal-to-noise ratio in the vehicle's carrier-tracking loop.

II. Carrier Suppression (Nonlinear PLL Theory)

If the phase modulation process is not Gaussian, the covariance function $K_\eta(\tau)$ is not mathematically tractable; however, the carrier-suppression factor may still be computed. From Chapter 2, Section III, the distribution of the phase estimate θ_1 is well approximated by

$$p(\theta_1) = \frac{\exp\left(\sigma_{\theta_1}^{-2}\cos\theta_1\right)}{2\pi I_0\left(\sigma_{\theta_1}^{-2}\right)}, \qquad |\theta_1| \leq \pi \tag{6-6}$$

where $\sigma_{\theta_1}^2$ is given by

$$\sigma_{\theta_1}^2 = \frac{N_{10}W_{L1}G^2}{2P_{c1}} \tag{6-7}$$

The term $\sigma_{\theta_1}^2$ is the variance as determined from the linear PLL theory.

The waveform $\eta(t)$ may be written as

$$\eta(t) = \sqrt{2P_{c2}}\cos\theta_1\cos\omega_{10}t + \sqrt{2P_{c2}}\sin\theta_1\sin\omega_{10}t \tag{6-8}$$

and the intensity of the carrier component becomes

$$I_c = \left[\sqrt{P_{c2}}\int_{-\pi}^{\pi}(\cos\theta_1 + \sin\theta_1)\,p(\theta_1)d\theta_1\right]^2 \tag{6-9}$$

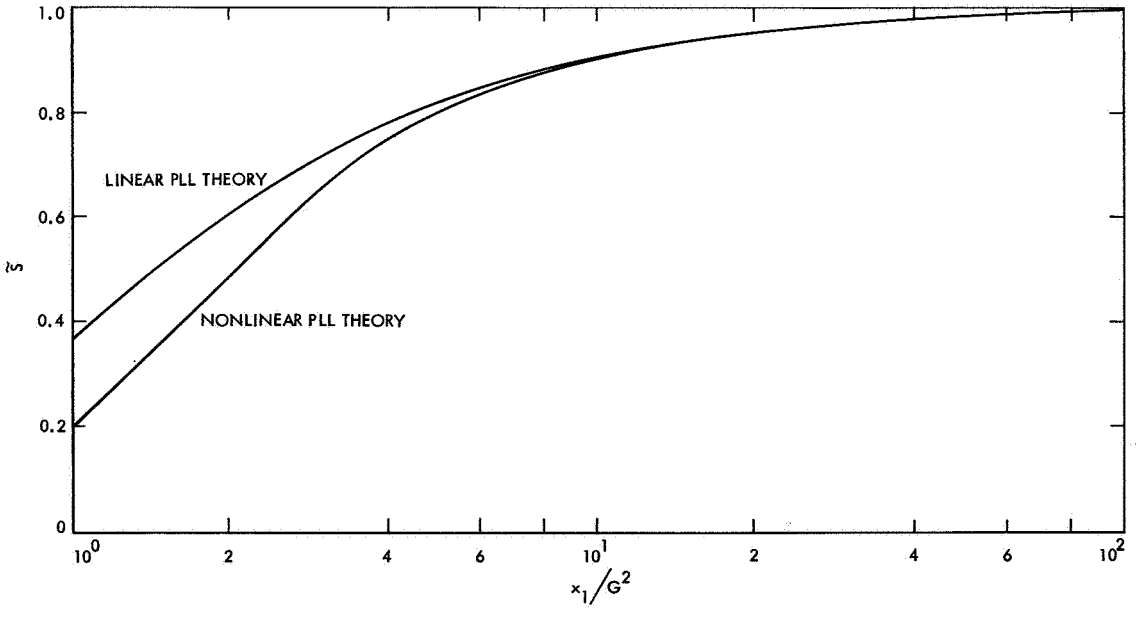

Fig. 6-1. Carrier suppression $\tilde{S}$ vs the parameter x_1/G^2; linear and nonlinear PLL theories are assumed and no BPLs are present

and, using Eq. (6-6), we reduce I_c to

$$\left.\begin{aligned} I_c &= P_{c2}\,[\overline{(\cos\theta_1)}]^2 \\ I_c &= P_{c2}\,\frac{I_1(\sigma_{\theta_1}^{-2})}{I_0(\sigma_{\theta_1}^{-2})} \end{aligned}\right\} \qquad (6\text{-}10)$$

The corresponding carrier suppression is given by

$$\tilde{S} = \frac{I_c}{P_{c2}} = \frac{I_1(\sigma_{\theta_1}^{-2})}{I_0(\sigma_{\theta_1}^{-2})} \qquad (6\text{-}11)$$

where $I_k(x)$ is the imaginary Bessel function of order k and argument x. The factor $\tilde{S}$ is plotted in Fig. 6-1 for comparison with that obtained using the linear PLL theory. Note that as $\sigma_{\theta_1}^{-2}$ approaches zero, the downlink carrier component is completely suppressed in the vehicle.

III. Carrier Suppression (Linear PLL Theory With BPLs Preceding the Loop)

Here we assume that the bandwidth of the vehicle's carrier-tracking loop is small enough for the process $\theta_1(t)$ to be Gaussian (i.e., the linear theory may be used). Thus, the variance of the process $\theta_1(t)$ adequately characterizes the carrier suppression.

From Chapter 3, Section I, the variance of θ_1, if we assume that $\theta_1 = 0$ without loss of generality, becomes

$$\sigma_{\theta_1}^2 = \left(\frac{N_{10}W_{10}}{2P_{c1}}\right) \times (G^2\Gamma_1) \times \left(\frac{1 + \frac{r_{10}}{\mu_1}}{1 + r_{10}}\right) \qquad (6\text{-}12)$$

and Γ_1 and μ_1 are defined in Eqs. (3-9) and (3-17), respectively. Thus, the downlink carrier suppression is given by

$$\tilde{S} = \exp\left(-\sigma_{\theta_1}^2\right) \qquad (6\text{-}13)$$

where $\sigma_{\theta_1}^2$ is defined in Eq. (6-12). In Fig. 6-2, this suppression is plotted against $2P_{c1}/N_{10}W_{10}G^2$ for various system mechanizations. In this figure, the parameter $x_1 = 2P_{c1}/N_{10}W_{10}$ is the signal-to-noise ratio that exists in the "design-point" loop bandwidth.

IV. Carrier Suppression (Nonlinear PLL Theory With PBLs Preceding the Loop)

In this case, the covariance $K_\eta(\tau)$ cannot be determined mathematically; however, on the basis of the results in Section II of this chapter and Eqs. (3-19) and (3-20),

$$\tilde{S} = \left[\frac{I_1(\alpha)}{I_0(\alpha)}\right]^2 \qquad (6\text{-}14)$$

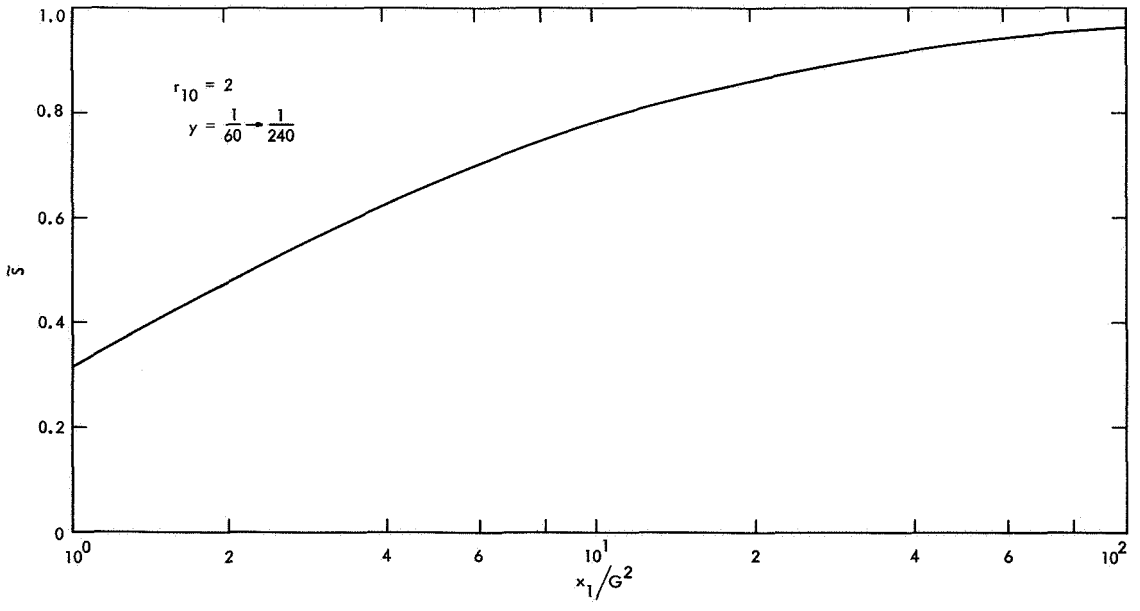

Fig. 6-2. Carrier suppression $\tilde{S}$ vs the parameter x_1/G^2; linear PLL theory is assumed and BPLs are present

where

$$\alpha = \frac{2P_{c1}}{N_{10}W_{10}} \times \frac{1}{\Gamma_1 G^2} \times \left(\frac{1 + r_{10}}{1 + \frac{r_{10}}{\mu_1}} \right) \qquad (6\text{-}15)$$

and Γ_1 and μ_1 are defined in Eqs. (3-9) and (3-17), respectively. As before, we note that the downlink carrier is completely suppressed when the uplink signal-to-noise ratio approaches zero. This result further supports the uniform distribution of $p(\phi_2)$ of Eq. (4-25) as α_2 approaches zero, and, further, supports the analytical model in this signal-to-noise ratio region. Plotted in Fig. 6-3 is Eq. (6-14) vs $x_1/G^2 = 2P_{c1}/N_{10}W_{L1}G^2$ for various system mechanizations. In this figure, the parameter $x_1 = 2P_{c1}/N_{10}W_{10}$ is the signal-to-noise ratio existing in the "design-point" loop bandwidth.

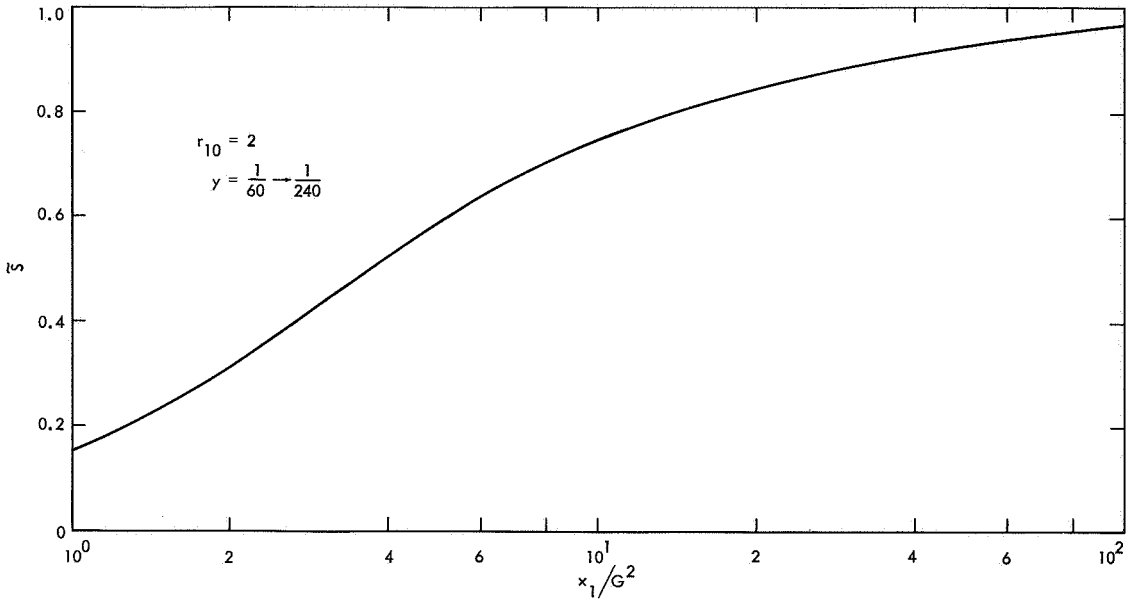

Fig. 6-3. Carrier suppression $\tilde{S}$ vs the parameter x_1/G^2; nonlinear PLL theory is assumed and BPLs are present

Reference

6-1. Middleton, D., *Introduction to Statistical Communication Theory*. McGraw-Hill Book Co., Inc., New York, 1960.

Chapter 7

Diversity Combining to Improve Radio-Frequency Phase and Doppler Measurements in One-Way and Two-Way Coherent Communication Systems

I. Introduction

Diversity is defined here as a general technique that utilizes two or more copies of a signal with varying degrees of disturbance to obtain, by a selection or combination scheme, a larger signal-to-noise ratio than is obtainable from either of the copies separately. Although diversity is commonly understood to be aimed at improving the reliability of reception of signals that are subject to fading in the presence of random noise, the significance of the term will be extended here to cover conceptually related techniques. In particular, these techniques are intended to reduce the effective phase and doppler error occurring in deep-space communication systems.

The first problem in diversity reception is the procurement of the "diverse" copies of the disturbed signal, or, if only one copy is available, the operation on this copy necessary to generate additional "diversified" copies. In space communications, the transmission medium can be tapped for an ever-available supply of diversified copies by employing more than one receiving antenna. If physically separated by several wavelengths, the observed signal copies will be statistically independent. Hence, the improvements due to diversity reception are realized. If, in fact, the copies are not statistically independent, the gain obtained is due only to an increase in antenna area.

The second problem in diversity is how to utilize the available disturbed copies of the signal to achieve the least possible loss of information in extracting the desired message or signal parameter. The technique of particular interest here is RF combining, i.e., *coherently* summing the observed copies at the observed frequencies. In practice, this is a difficult feat; however, in what follows we will assume that this can be accomplished with perfect precision.

II. Improvements Realized in RF Phase Measurements With Use of Diversity Techniques

Denote the output of the ℓth antenna ($\ell = 1, 2, \cdots, L$) by

$$\xi_\ell(t) = \sqrt{2P_{c2}} \sin [\omega_{2\ell} t + \hat{\theta}_{1\ell} + \theta_{2\ell}] + n_{2\ell}(t) \tag{7-1}$$

where $\omega_{2\ell}$ is the radian frequency of the carrier component, $\theta_{1\ell}$ is the phase jitter on the downlink carrier due to the additive noise on the uplink, $\theta_{2\ell}$ is the phase shift on the downlink, and $n_{2\ell}(t)$ is white Gaussian noise of single-sided spectral density N_{20} W/Hz. Thus, the observed waveform appearing at the output of the RF combination is given by

$$\xi(t) = \sum_{\ell=1}^{L} \xi_\ell(t)$$

which becomes, when we use Eq. (7-1) and the facts that $\hat{\theta}_{1\ell} = \hat{\theta}_1$, $\theta_{2\ell} = \theta_2$, and $\omega_{2\ell} = \omega_2$ for all values of $\ell = 1, 2, \cdots, L$,

$$\xi(t) = \sqrt{2L^2P_{c2}} \sin [\omega_2 t + \hat{\theta}_1 + \theta_2] + n_{2L}(t) \tag{7-2}$$

where $n_{2L}(t)$ is white Gaussian noise of single-sided spectral density LN_{20} W/Hz. Thus, RF combining has increased the signal power by a factor of L^2 watts while the noise power per unit bandwidth is increased by the factor L watts.

We may determine the variance of the two-way tracking phase error using the theory and results given in Chapter 4, i.e.,

$$\sigma^2_{\phi_{r2}} = \frac{1}{\alpha_1} + \frac{1}{\alpha_2} \tag{7-3}$$

where

$$\alpha_1 = \frac{2P_{c1}}{W_{L1}N_{10}} \times \frac{1}{G^2K_R(r_1, r_2, \beta)}, \qquad \alpha_2 = \frac{2LP_{c2}}{N_{20}W_{L2}} \tag{7-4}$$

and $K_R(r_1, r_2, \beta)$ is defined in Eq. (4-20). Further, the statistics of the two-way-tracking phase-error distribution are well approximated if we use Eq. (4-25) and the α_1 and α_2 as defined in Eq. (7-4).

Where BPLs precede the carrier-tracking loops, the variance of the phase error, as determined from the linear PLL theory, is given by

$$\sigma^2_{\phi_{r2}} = \frac{1}{\alpha_{1\ell}} + \frac{1}{\alpha_{2\ell}} \tag{7-5}$$

where

$$\left.\begin{aligned} \alpha_{1\ell} &= \frac{2P_{c1}}{N_{10}W_{10}} \times \frac{1}{G^2\Gamma_1K_R(k_1, k_2, \beta)} \\ \alpha_{2\ell} &= \frac{2LP_{c2}}{N_{20}W_{20}} \times \left(\frac{1 + r_{20}}{1 + \frac{r_{20}}{\mu_2}}\right) \frac{1}{\Gamma_2} \end{aligned}\right\} \tag{7-6}$$

and Γ_1 and $K_R(k_1, k_2, \beta)$ are defined in Eqs. (4-33) and (4-35) respectively. The factor Γ_2 is given by

$$\Gamma_2 = \frac{1 + 0.345Lx_2y_2}{0.862 + 0.690Lx_2y_2} \tag{7-7}$$

where x_2 and y_2 are defined in Eq. (4-33). On the other hand, the model of the phase-error distribution, employing the nonlinear PLL theory with BPLs preceding the carrier-tracking loops and with L-fold diversity, is well approximated by Eq. (4-36) with $\alpha_{1\ell}$ and $\alpha_{2\ell}$ given in Eq. (7-6). Thus, the design of an L-fold, RF combining, diversity phase-measuring system may proceed on the basis of the formulas given in this section.

III. Improvements Realized in One-Way- and Two-Way-Doppler Measurements With Use of Diversity Techniques

Using the linear PLL theory of Chapter 5, we can easily show the variance of the two-way-doppler error to be

$$\sigma^2_{\phi_d} = \frac{1}{d_1} + \frac{1}{d_2} \tag{7-8}$$

where

$$d_1 = \frac{2P_{c1}}{N_{10}W_{L1}} \times \frac{1}{G^2K_D(r_1, r_2, \beta)}, \qquad d_2 = \frac{2P_{c1}L}{N_{20}W_{L2}} \tag{7-9}$$

and $K_D(r_1, r_2, \beta)$ is defined in Eq. (5-13). The statistics of the two-way-doppler error are determined from

Eq. (5-16) where d_1 and d_2 are given in Eq. (7-8), i.e.,

$$p(\phi_d) = \frac{I_0(\,|\,d_1 + d_2 \exp(j\phi_d)\,|\,)}{2\pi I_0(d_1) I_0(d_2)}, \qquad |\,\phi_d\,| \leq \pi \tag{7-10}$$

This, of course, is a result of the nonlinear PLL theory.

When BPLs precede the carrier-tracking loops, the variance of the two-way-doppler is given by

$$\sigma^2_{\phi_d} = \frac{1}{d_{1\ell}} + \frac{1}{d_{2\ell}} \tag{7-11}$$

where

$$\left.\begin{aligned} d_{1\ell} &= \frac{2P_{c1}}{W_{10}N_{10}} \times \frac{1}{G^2\Gamma_1 K_D(k_1, k_2, \beta)} \\ d_{2\ell} &= \frac{2LP_{c2}}{N_{20}W_{20}\Gamma_2} \times \left(\frac{1 + r_{20}}{1 + \frac{r_{20}}{\mu_2}}\right) \end{aligned}\right\} \tag{7-12}$$

This is easily determined if we use the linear PLL theory given in Chapter 3 and the results from Chapter 5. The functions Γ_1, and $K_D(k_1, k_2, \beta)$ are defined in Eqs. (4-33) and (5-22), respectively, and Γ_2 is defined by Eq. (7-7). Finally, for L-fold diversity, the statistics of the two-way-doppler error are well approximated by Eq. (5-23) if we use Eq. (7-12) to specify $d_{1\ell}$ and $d_{2\ell}$. This distribution is, of course, a model two-way-doppler error when BPLs precede the carrier-tracking loops and the nonlinearities of the PLLs are considered. Thus, the design of an L-fold, RF combining, doppler measuring system may proceed on the basis of the formulas given in this section.

IV. Conclusions

The reliability of a communication system employing antenna diversity to measure the RF phase-error and doppler shift is basically determined by the properties of the signal at the receiving site and by the operating condition of the combining equipment. Accordingly, we have concentrated in the present chapter on the effect of diversity upon signal reliability, and have ignored the equally important topic of equipment reliability. In any case, the design of an L-fold, RF combining, diversity system may proceed on the basis of the linear or nonlinear PLL theory developed in this chapter and, by replacing P_{c2} with LP_{c2}, the curves given in Chapters 4 and 5. If BPLs are used, as is the case in practice, the design then must be predicated upon the development given in this chapter. The reason, of course, that the curves in Chapters 4 and 5 do not apply in this case is that the limiter performance factor Γ_2 depends upon L, and this fact has not been taken into consideration in Chapters 3 and 4 (i.e., $L = 1$). The results derived in this chapter assume a common gain among the L antennas.

Nomenclature

d_1 doppler variable characterizing the distribution $p(\phi_d)$ in a one-way system

d_2 doppler variable characterizing the distribution $p(\phi_d)$ in a two-way system

$F(s)$ linear loop-filter transfer function

G static phase gain of the vehicle's carrier-tracking loop

$H(s)$ closed loop transfer function of the linearized second-order loop

I_c intensity of the downlink carrier component, W

$\mathrm{I_k(x)}$ imaginary Bessel function of order k and argument x

$\mathrm{I_0(x)}$ imaginary Bessel function of order zero and argument x

K $K_i K_m K_{\mathrm{VCO}}$, equivalent simple-loop gain, $\mathrm{V^{-1}\,s^{-1}}$

L diversity order

$K_D(k_1, k_2, \beta)$ doppler coefficient

K_1 rms VCO signal output

K_m mixer gain, $\mathrm{V^{-1}}$

K_{VCO} VCO gain constant, rad/s–V

L diversity order

$n = 1$ refers to uplink parameters

$n = 2$ refers to downlink parameters

N_0 single-sided noise spectral density, W/Hz

N_{n0} single-sided spectral density of the additive noise ($n = 1$ or 2), W/Hz

p Heaviside operator, d/dt

$p(\phi_d)$ probability density function of the doppler error

$p(\phi_2)$ probability distribution of the two-way phase error

P signal power into loop, W

P_{cn} power remaining in the carrier component ($n = 1$ or 2), W

P_n total radiated power ($n = 1$ or 2), W

r second-order loop parameter ratio equal to $K\tau_2^2\sqrt{P}/\tau_1$ without a BPL, and equal to $\alpha_l K\tau_2^2/\tau_1$ with a BPL

r_{n0} second-order loop natural frequency, Hz

s Laplace transform variable

$\bar{S}$ total average number of phase jumps per unit of time

$\tilde{S}$ carrier suppression factor

$S_l(s)$ spectral density of noise at limiter output, W/Hz

w_l noise bandwidth of the limiter output spectrum, Hz

W_i single-sided bandwidth of the IF filter, Hz

W_L dynamic double-sided linear loop bandwidth ($W_L = 2B_L$), Hz

W_{Ln} dynamic double-sided bandwidth of the carrier-tracking loop, Hz

W_{L0} double-sided loop bandwidth at "design point" or loop threshold ($W_{L0} = 2B_{L0}$), Hz

W_{n0} double-sided bandwidth of the carrier-tracking filter ($n = 1$ or 2), Hz

x signal-to-noise ratio in bandwidth of the loop, $2P/N_0\,W_L$

x_n signal-to-noise ratio existing in the carrier-tracking-loop bandwidth, $2P_{cn}/N_{n0}W_{n0}$ or $P_{cn}/N_{n0}B_{n0}$

y ratio of loop bandwidth to IF-filter bandwidth, W_L/W_i

α loop signal-to-noise ratio in W_L

α_l limiter signal–voltage suppression factor

α_{l0} limiter signal–voltage suppression factor at system "design point", or value of α_l at threshold

β ratio of loop bandwidths

Γ limiter suppression factor, α_{l0}/α_l

ζ_n linear loop damping factor

η xy

η_l input signal-to-noise ratio of the limiter, $2P/N_0W_i$

$\theta_l(t)$ arbitrary phase shift of Lth diversity path

μ limiter suppression factor, α_{l0}/α_l

σ^2 variance of loop phase error, linear PLL theory

Nomenclature (contd)

σ_{d1}^2 mean-squared value of one-way doppler error

σ_{d2}^2 mean-squared value of two-way doppler error

σ_{ϕ}^2 variance of loop phase error, rad^2

$\sigma_{\phi_1}^2$ variance of the one-way phase-measurement error

$\sigma_{\phi_2}^2$ variance of the two-way phase-measurement error

τ_1 second-order loop denominator time constant of $F(s)$, s

τ_2 second-order loop numerator time constant of $F(s)$, s

$\phi(t)$ phase error in loop, rad

ϕ_1 phase error in the one-way system, rad

ϕ_2 phase error in the two-way system, rad

ω_0 quiescent frequency of the VCO, rad/s